Am J Transl Res 2020;12(10):6723-6739
www.ajtr.org /ISSN:1943-8141/AJTR0113151

Original Article

Notch signaling mitigates chemotherapy toxicity by accelerating hematopoietic stem cells proliferation via c-Myc

Juanjuan Chen[1,2*], Yan Dong[3*], Jie Peng[1], Jian Zhang[1], Xiaotong Gao[3], Aili Lu[1], Chunlin Shen[1]

[1]*State Key Laboratory of Organ Failure Research, Guangdong Provincial Key Laboratory of Viral Hepatitis Research, Department of Infectious Diseases, Nanfang Hospital, Southern Medical University, Guangzhou, China;* [2]*Department of Oncology and Hematology, 421th Hospital of Chinese People's Liberation Army, Guangzhou, China;* [3]*Department of Hematology, Tangdu Hospital, Fourth Military Medical University, Xi'an, China.* [*]*Equal contributors.*

Received April 5, 2020; Accepted September 22, 2020; Epub October 15, 2020; Published October 30, 2020

Abstract: The mechanisms that regulate hematopoietic stem cell (HSC) regeneration after myelosuppressive injury are not well understood. Here, we showed that disruption of Notch signaling aggravated chemotherapy-induced myelosuppression in inducible genetic mice. Conversely, Notch activation correlated positively with clinical HSC engraftment. We used endothelial-targeted chimeric Notch ligand Delta-like 1 (D1R) to activate Notch signaling in hematopoietic stem/progenitor cells through micro-environmental cellular contact. Recombinant protein D1R contributed to the recovery of the HSC pool and sustained HSC vitality in response to various chemotherapeutic agents *in vivo*. Mechanistically, D1R treatment promoted HSC proliferation transiently, prevented HSC exhaustion, correlated with activation of the downstream phosphoinositide 3-kinase (PI3K)/extracellular-signal-regulated kinase (ERK)/BCL2 associated agonist of cell death (BAD) signaling axis during regeneration, and partially mediated upregulation of c-Myc in HSCs. These data reveal an unrecognized role for Notch signaling in promoting HSC repopulation after myelosuppressive chemotherapy and offer a new therapeutic approach to mitigate chemotherapy-induced injury.

Keywords: Hematopoietic stem cells regeneration, notch signaling, delta-like 1, proliferation, c-Myc

Introduction

Hematopoiesis is a continuous process of blood cell production that occurs through the orchestrated self-renewal, proliferation, and differentiation of hematopoietic stem cells (HSCs). HSCs are the only cells capable of producing all blood cell lineages. Deficient hematopoiesis, which is characterized by pancytopenia, occurs when the regeneration and multi-lineage differentiation potential of HSCs is damaged by high-dose chemotherapy or radiation. This condition is a life-threatening complication for most cancer patients. Although several growth factors show single lineage reconstructive properties in the clinic, few are effective in regulating the multi-lineage differentiation of HSCs. A new strategy to protect the HSC pool and resume hematopoiesis from myeloablative injury induced by antineoplastic therapy is a substantial unmet clinical need.

HSCs are maintained in the bone marrow (BM) microenvironment (niche), which includes specialized niche cells that produce pro-hematopoietic factors [1]. Crosstalk between various niche cells and HSCs is indispensable for HSC homeostasis and regeneration. Most HSCs localize adjacent to sinusoidal blood vessels (perivascular niche), demarcated by BM sinusoidal endothelial cells (ECs) [2-4]. It has been strongly implicated that thin walled, fenestrated ECs can provide the proper milieu of pro-hematopoietic signals needed to support the HSCs, including Notch signaling [5, 6].

Canonical Notch signaling activation is mediated by Notch ligand-receptor interaction. There are five Notch ligands (Delta-like 1, Delta-like 3, Delta-like 4, Jagged 1, and Jagged 2) and four receptors (Notch 1, Notch 2, Notch 3, and Notch 4) in mammals. The Delta-Serrate-Lag-2 (DSL) domain of the ligands triggers the release

of Notch intracellular domain (NICD) from the receptor. NICD then translocates into the nucleus and associates with the recombination signal binding protein Jκ (RBP-J) to transactivate downstream genes such as Hes and Hey family members [7]. We previously demonstrated that, in the hematopoietic cell-microenvironment, Notch interactions are critical for HSC expansion and regeneration, particularly myeloid reconstruction under homeostasis and radiation insult, respectively [7, 8]. Therefore, we hypothesized that Notch signaling might also contribute to hematopoietic regeneration after chemotherapeutic injury.

Here, we used conditional deletion of RBP-J in marrow hematopoietic cells to confirm that Notch loss-of-function transgenic mice exhibit a strongly deteriorated hematopoietic reconstitution after chemotherapy. The correlation between Notch activation and graft function in hematopoietic stem cells transplantation (HSCT) patients further verified the positive role of Notch signaling in myelosuppression. In addition, pharmacologic activation of Notch signaling through the EC-targeted soluble recombinant protein D1R improved multi-lineage hematopoietic reconstitution by transiently accelerating HSC proliferation during early stages of BM regeneration in chemotherapeutic stress situations *in vivo*, which was mediated by activation of the downstream phosphoinositide 3-kinase (PI3K)/extracellular-signal-regulated kinase (ERK)/BCL2 associated agonist of cell death (BAD) signaling axis, and at least partially due to the D1R-mediated upregulation of c-Myc in HSCs. Expanded HSCs showed a robust competitive transplantation advantage at later stages. Collectively, these data revealed a novel role for Notch signaling to sustain hematopoietic stem/progenitor cell (HSPC) reconstitution in situations of acute chemotherapeutic stress. Notch-regulated HSPC proliferation continued until the HSC pool recovered, thereby preventing hematopoietic exhaustion during myelotoxic stress. Modulating Notch signaling between HSCs and niche cells could lead to the discovery of a new pancytopenia treatment after chemotherapy.

Materials and methods

Mice and poly(I)-poly(C) treatment

Adult 8-week-old male mice were used throughout the study and maintained under specific-pathogen-free conditions. Mx1-Cre, RBP-J$^{f/f}$, Mx1-Cre-RBP-J$^{f/f}$ and Mx1-Cre-RBP-J$^{f/+}$ mice have been described previously with C57BL/6 background [9]. Homozygous and heterozygous transgenic mice were intraperitoneally injected with poly(I)-poly(C) (Sigma-Aldrich) to induct RBP-J deletion in hematopoietic cells as described previously [9]. All animal procedures were performed in accordance with the detailed rules for the administration of animal experiments for medical research purposes issued by the Ministry of Health of China and were approved by the Animal Care and Use Committees of the Southern Medical University, Guangzhou, China.

Cytotoxic agents in vivo administration

C57BL/6, Mx1-Cre-RBP-J$^{f/f}$ and Mx1-Cre-RBP-J$^{f/+}$ mice were intraperitoneally injected with cyclophosphamide (CTX, 150 mg/kg, Sigma-Aldrich), 5-fluorouracil (5-FU, 150 mg/kg, Sigma-Aldrich) or cisplatin (5 mg/kg, Sigma-Aldrich). Mice were intraperitoneally injected with D1R (4 mg/kg) or equivalent phosphate-buffered saline (PBS) daily for 7 or 14 days post chemotherapy as required [7].

Fluorescence-activated cell sorting

Fluorescence-activated cell sorting (FACS) analysis was performed on FACSCalibur™ or FACSAriaII flow cytometer (BD Immunocytometry Systems). The information about antibodies were listed in Table S1. Data were analyzed with the FlowJo vX.0.6 software. To monitor cell proliferation *in vivo*, 5-bromo-2'-deoxyuridine (BrdU, Sigma-Aldrich) was administered intraperitoneally every 2 days (100 mg/kg) after chemotherapy and maintained in drinking water (1 mg/ml) for 7 days. Cell cycle was performed using PI staining. Apoptosis was analyzed with Annexin V Apoptosis Detection Kit (eBioscience).

Immunofluorescence assay

The volunteers and HSCT patients peripheral blood cells were centrifugally added onto slides and fixed with 4% polyformaldehyde. The slides were dried at room temperature, blocked with fetal bovine serum, and incubated with intracellular domains of Notch 1 (ICN1) primary antibody (dilution 1:50, Santa Cruz) overnight at 4°C, followed by incubation with a FITC-conjugated secondary antibody (dilution 1:200,

Invitrogen). The cell nuclei were counterstained with Hoechst33258. Images were performed using a laser confocal microscope (FV1000, Olympus). All subjects gave their informed consent for inclusion before they participated in the study. The study was approved by the Ethics Committee of 421th Hospital of Chinese People's Liberation Army, and written informed consent was obtained from all subjects, in compliance with the Declaration of Helsinki.

Colony forming unit assay

Isolated bone marrow nucleated cells were plated in Methocult 3434 (STEMCELL Technologies) for 14 days. Colonies consisting of > 50 cells were counted using a microscope.

Competitive bone marrow transplantation

5×10^5 bone marrow cells from D1R or PBS treated GFP mice at day 7 after CTX injection were collected and co-transplanted with 5×10^3 congenic competing BM cells into irradiated C57BL/6 mice (single 1000 cGy ^{60}Co γ-ray total body irradiation), through tail vein injection. Blood chimerism was monitored monthly. Mice were kept for 8 weeks.

Gene expression analysis

RNA was isolated with TRIzol reagent (Invitrogen), and was reverse transcribed to cDNA (Takara). Quantitative real-time PCR (qRT-PCR, Takara) was performed in ABI Prism 7500 Real-Time PCR System, with β-actin been used for normalization. The primers were listed in Table S2.

Western blotting

LSK ($Lin^-Sca\text{-}1^+c\text{-}Kit^+$) cells from D1R or PBS treated chemotherapeutic mice were lysed with RIPA buffer at day 7 after CTX exposure, and subsequently incubated with primary antibodies against PI3K, Erk1/2, pErk1/2, Bad, pBad, Bax, Bcl-2 and β-actin. The secondary antibodies were peroxidase-conjugated anti-rabbit IgG or anti-mouse IgG.

Lentivirus transfection

Expanded LSK cells were transfected using a pGV118-U6-shRNA-Ubi-EGFP lentivirus packaging, with c-Myc or empty vector, and further cultured in serum-free medium (StemSpan SFEM) supplemented with 20 ng/mL thrombopoietin, 125 ng/mL stem cell factor, 50 ng/mL Flt-3 ligand, 25 ng/mL interleukin-6 and 10 ng/mL interleukin-3 for 7 days. Quantitative real-time PCR was performed to confirm c-Myc knock-down. Lethally irradiated C57BL/6 recipient mice were administered 5×10^3 LSK cells mixed with 5×10^5 competing marrow mononuclear cells, via tail vein injection.

Statistical analysis

All data are recorded as mean ± standard error of mean (SEM) and analyzed using SPSS Statistics 20.0 (IBM, Armonk, New York, US). Comparisons between two groups were determined using the students t-test for normally distributed values and the Mann-Whitney-U-test for non-normally distributed values. One-way analysis of variance (ANOVA) was used to evaluate differences of measurement data among groups. Survival was analyzed by Kaplan-Meier analysis. Differences were considered significant at the level of $P < 0.05$. GraphPad Prism 6.0 software was used for graphical representation.

Results

Notch signaling blockade aggravates chemical-induced myelosuppression

To determine the naive role of canonical Notch signaling in myelosuppressive chemotherapy, we treated C57BL/6 mice with or without cyclophosphamide (CTX) to measure Notch signaling activity in BM Lin^- cells following chemotherapy. Comparison of Hes1, Hes5, Hey1, Hey2, and Delta-like 1 expression demonstrated no statistical differences compared to untreated mice (Figure S1A), indicating that CTX did not influence the Notch pathway in HSPCs.

We generated Mx1-Cre-RBP-$J^{f/f}$ and Mx1-Cre-RBP-$J^{f/+}$ mice and induced homozygous (cKO) and heterozygous (Ctrl) RBP-J disruption by injection of poly(I)-poly(C). RBP-J cKO mice showed no statistically significant alterations in survival but did exhibit a significant decrease in total mononuclear cells from the bilateral femur BM, spleen, and peripheral blood at day 7 following CTX compared with Ctrl mice (**Figure 1A**). In addition, flow cytometry analysis of $Lin^-Sca\text{-}1^+c\text{-}Kit^+$ (LSK) cells from the BM and spleen confirmed a robust aggravation in RBP-J cKO

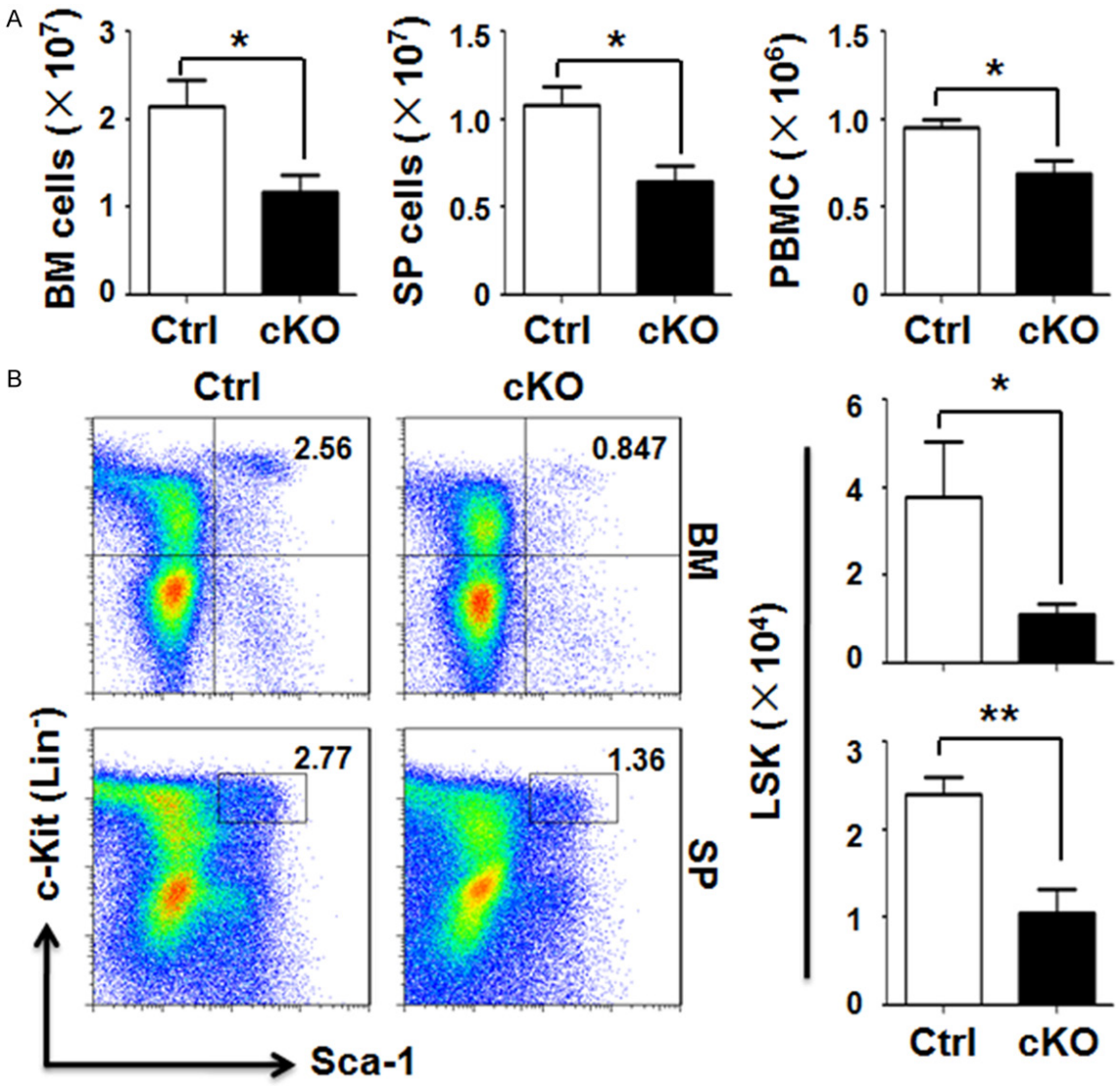

Figure 1. Notch signaling blockade aggravates chemical-induced myelosuppression. A. Total mononuclear cells of bome marrow (BM), spleen (SP) and peripheral blood mononuclear cells (PBMCs) from Mx1-Cre-RBP-J$^{f/f}$ (cKO) and Mx1-Cre-RBP-J$^{f/+}$ (Ctrl) mice 7 days after 150 mg/kg CTX treatment. B. Representative FACS profiles (left) and numbers (right) of BM and spleen LSK (Lin$^-$Sca-1$^+$c-Kit$^+$) cells in cKO and Ctrl mice 7 days after CTX. Data are presented as the means ± SEM (n=6). *P < 0.05, **P < 0.01 vs Ctrl.

mice (**Figure 1B**). Consistent with previous reports [10], inactivation of Notch signaling blocked T cell development (Figure S1B) and myeloid lineage differentiation (Figure S1C). These data demonstrate that disruption of Notch signaling blocked hematopoietic reconstitution following a myelosuppressive-dose of CTX, particularly in the stem cell pool.

Notch activation correlates with graft function in HSCT

To assess whether Notch signaling was active in myeloablative chemotherapy patients, we examined the nuclear localization expression of Notch 1 intracellular domain transcription factor (ICN1) in peripheral blood mononuclear cells from healthy volunteers and allogeneic hematopoietic stem cell transplantation (allo-HCT) patients. Poor graft function (PGF) is defined as a failure to achieve two or three adequate blood counts (absolute neutrophil count ≤ 0.5 × 10^9/L, platelet counts ≤ 20 × 10^9/L, or hemoglobin ≤ 80 g/L) by day 28 following allo-HCT in the presence of complete donor hematopoiesis [11]. All healthy individuals and pretransplant patients displayed similar ICN1 nucleus expression; however, ICN1 was enri-

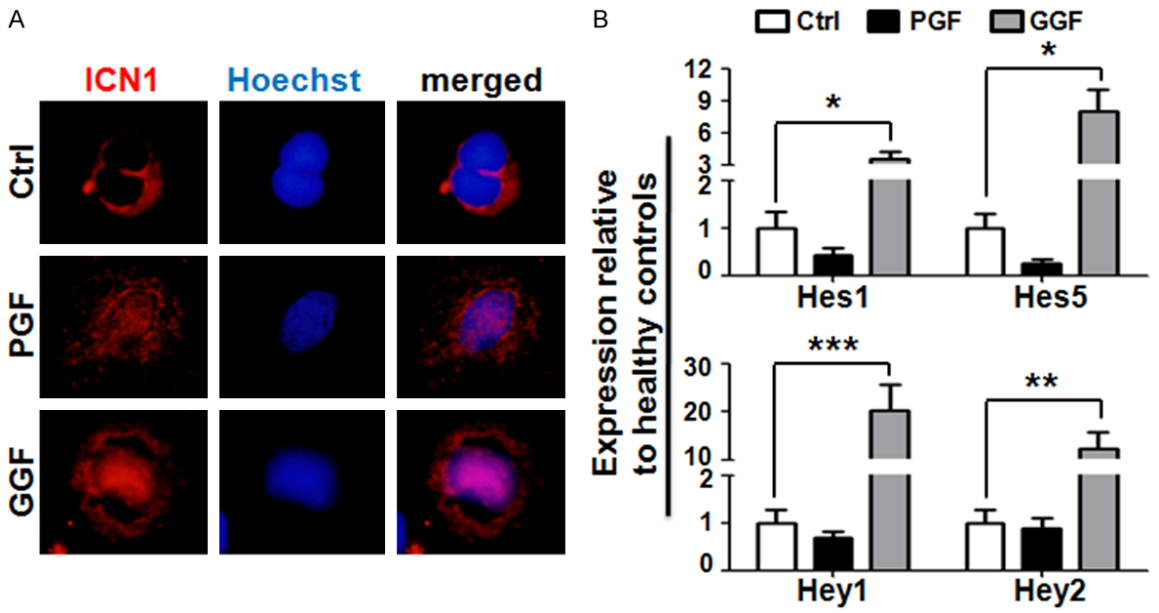

Figure 2. Notch activation correlates with graft function in HSCT. A. PBMCs stained with ICN1 (red) and Hoechst (blue) at two weeks after allo-HCT, from healthy human volunteers (Ctrl, n=10) and allo-HCT patients either with good graft function (GGF, n=18) or poor graft function (PGF, n=13). B. Quantitative RT-PCR analysis of Hes1, Hes5, Hey1 and Hey2 in PBMCs at two weeks after allo-HCT, from healthy human volunteers (Ctrl) and allo-HCT patients with GGF or PGF. Data are presented as the means ± SEM. $*P < 0.05$, $**P < 0.01$, $***P < 0.001$ vs Ctrl.

ched in good graft function (GGF) patients compared to PGF patients 2 weeks after allo-HCT (**Figure 2A**). Consistently, modest upregulation of Notch signaling molecules, specifically Hes1, Hes5, Hey1, and Hey2, was observed in post-transplant GGF patients (**Figure 2B**). These clinical results indicated that Notch signaling might positively correlate with the engraftment post-allotransplant.

Notch signaling promotes BM reconstitution following CTX

To activate Notch signaling pharmacologically, we developed a fusion protein, D1R, composed of the Notch ligand Delta-like I DSL domain and an arginine-glycine-aspartic acid (RGD) motif to target niche ECs [7]. Following CTX chemotherapy, C57BL/6 mice receiving D1R daily showed a robust ICN1 nuclear expression in BM LSK cells in comparison to phosphate buffered saline (PBS)-treated mice (**Figure 3A**). Consistent with this observation, LSK cells revealed similar increased expression of Hes1 and Hes5 within 7 days following D1R administration (Figure S2A). These studies showed that Notch ligand recombinant protein D1R effectively activated Notch signaling in BM HSPCs.

Consistent with the temporary splenomegaly and hepatomegaly (**Table 1** and **Figure 3B**), rapid recovery of total mononuclear cells in bilateral femur BM, spleen, and peripheral blood was observed in D1R-treated mice 7 days following CTX treatment (**Table 1**). However, the difference returned to near-normal at day 14 (**Table 1**). Notably, myelogenesis recovered more quickly in D1R-treated mice (**Table 1** and Figure S2B). Consistent with flow cytometry results, a colony-forming assay revealed that D1R-treated mice demonstrated larger numbers and greater sizes of myeloid colonies, including BM-derived GM-, M-, and G-colony forming unit (CFU) (**Figure 3C**). There were no differences in granulocyte/monocyte progenitor (GMP), common myeloid progenitor, and myeloid/erythroid progenitor numbers, but the GMP proportion was mildly increased in D1R-treated animals (**Figure 3D**). Taken together, these results suggest pharmacologic activation of Notch signaling accelerated hematopoietic reconstitution after CTX myelosuppression, with a bias toward myelogenesis.

Notch signaling improves HSC regeneration following CTX

We next investigated whether D1R could affect the HSC phenotype after CTX chemotherapy. D1R administration significantly elevated the percentage and the number of LSK cells in both the BM and spleen (**Table 1** and Figure S3A).

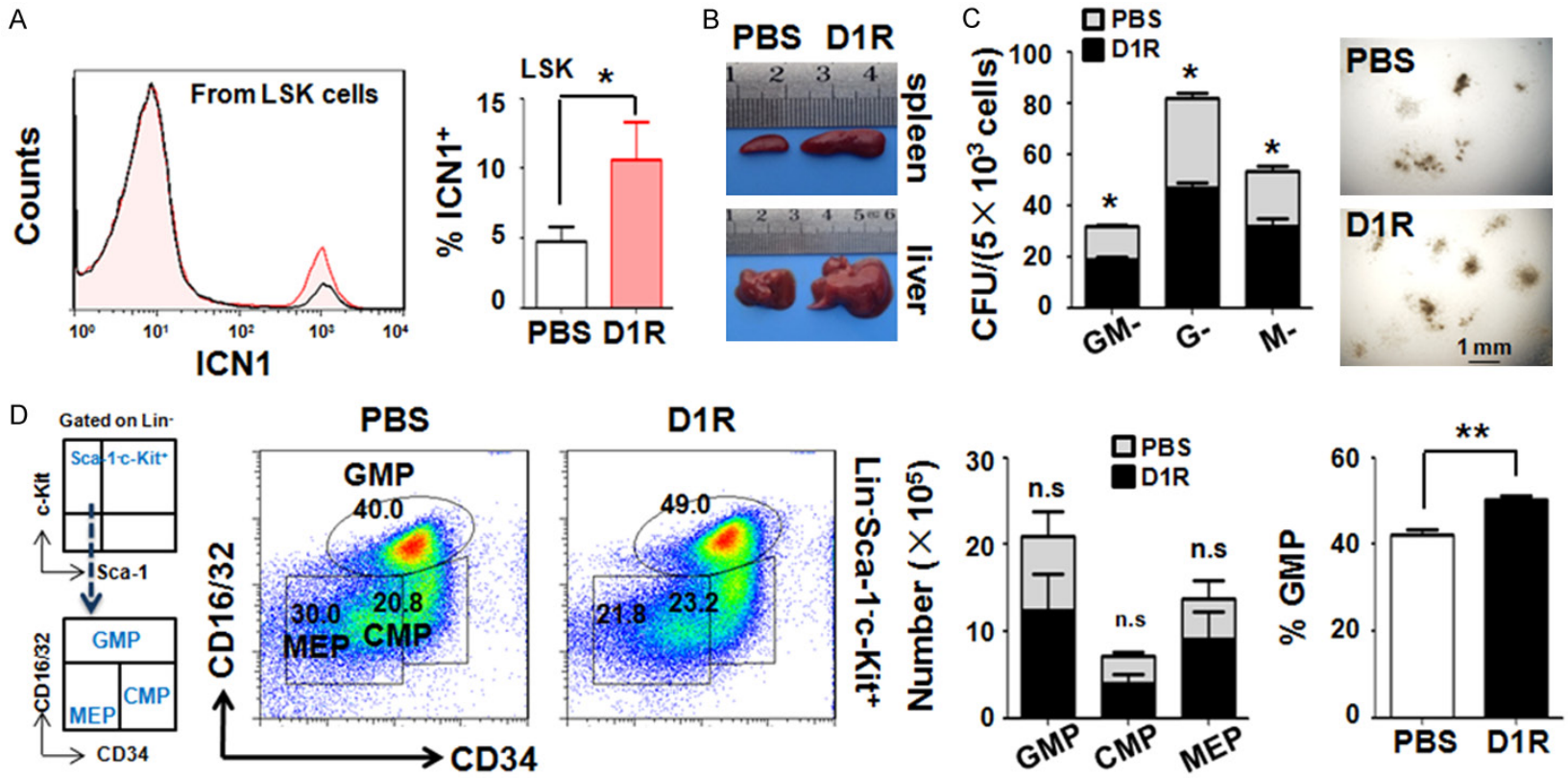

Figure 3. Notch signaling promotes BM reconstitution following CTX. 8-week-old C57BL/6 mice were daily injected with D1R (4 mg/kg) or equivalent PBS for 7 days following CTX. A. Representative FACS profiles (left) and rate (right) of intracellular staining of ICN1 in BM LSK cells. B. Pictures of spleen and liver 7 days after CTX. C. GM-, G- and M-CFU colonies (left) and representative images (right) of BM cells. D. Representative plots (left), numbers (middle) and percentage (right) of granulocyte/monocyte progenitors (GMP), common myeloid progenitors (CMP) and myeloid/erythroid progenitors (MEP) at 7 days following CTX. Bars, 1 mm. Data are presented as the means ± SEM (n=6). **P* < 0.05, ***P* < 0.01 vs PBS.

Table 1. Notch signaling promotes BM reconstitution following CTX

	day 7			day 14		
	PBS	D1R	*P* Value	PBS	D1R	*P* Value
BM cells (× 10^7)	4.69±1.63	6.90±1.93	0.019*	4.44±0.55	6.47±0.50	NS
Spleen cells (× 10^7)	0.89±0.28	2.90±0.32	0.009**	3.47±0.50	5.84±1.31	NS
PBMC (× 10^6)	0.45±0.05	1.99±0.30	0.044*	1.45±0.13	2.55±0.15	0.005**
Spleen/body weight (%)	0.35±0.02	0.94±0.14	0.044*	0.67±0.05	0.97±0.13	NS
Liver/body weight (%)	4.78±0.11	6.47±0.41	0.045*	5.32±0.11	5.84±0.32	NS
LSK in BM (× 10^5)	1.01±0.20	13.7±3.58	0.024*	1.44±0.21	2.92±0.20	0.007**
LSK in spleen (× 10^5)	0.30±0.04	18.5±3.30	0.032*	1.96±0.10	3.85±0.77	NS
$Ly6G^+CD11b^+$ cells in BM (× 10^6)	43.3±16.5	61.4±17.2	0.012*	19.9±3.37	33.6±2.00	0.025**
$Ly6G^+CD11b^+$ cells in SP (× 10^6)	2.37±0.44	17.5±2.67	0.005**	19.0±3.47	28.1±8.02	NS
$Ly6G^+CD11b^+$ cells in PBMC (× 10^6)	0.41±0.07	1.43±0.27	0.023*	0.60±0.12	1.00±0.13	NS

8-week-old C57BL/6 mice were daily injected with D1R (4 mg/kg) or equivalent PBS for 14 days after CTX treatment. Total nucleated cells, LSK cells and myeloid cells in the BM, spleen and PBMC were performed by FACS. Data are presented as the means ± SEM (n=6). *$P < 0.05$, **$P < 0.01$ vs PBS.

Specifically, D1R treatment resulted in increased numbers (**Figure 4A**) of long-term HSCs (LT-HSCs, $Lin^-Sca\text{-}1^+c\text{-}Kit^+CD48^-CD150^+$), short-term HSCs (ST-HSCs, $Lin^-Sca\text{-}1^+c\text{-}Kit^+CD48^-CD150^-$), and multipotent progenitor cells (MPPs, $Lin^-Sca\text{-}1^+c\text{-}Kit^+CD48^+CD150^-$).

To evaluate the long-term repopulating potential of HSCs, we further generated competitive chimeras by transplanting BM cells from D1R- or PBS-treated chemotherapeutic GFP mice into lethally irradiated C57BL/6 mice. A greater proportion of primary donor engraftment in both the BM and peripheral blood persisted in D1R-treated mice, with a corresponding increase of myeloid and B cell lineages (**Figures 4B** and S3B). Analysis of the percentage of GFP^+ LSK cells further confirmed that this difference was potentially related to HSC reconstitution (**Figure 4C**). Collectively, these data revealed that pharmacological activation of Notch signaling by D1R drove the protection and recovery of HSC compartments, particularly LT-HSCs.

To assess that the positive role of D1R is mediated through HSPC-specific Notch activation, a colony-forming cell methylcellulose assay was performed in D1R- or PBS-treated Mx1-Cre-RBP-$J^{f/f}$ and Mx1-Cre-RBP-$J^{f/+}$ mice in the context of CTX chemotherapy. We detected no difference in total CFU in RBPJ-deficient mice whether injected with D1R or with PBS (**Figure 4D**). These data suggest that D1R participated in hematopoietic regeneration at least partially by activating HSPC Notch signaling directly in response to a myelosuppressive stressor.

Notch signaling restores hematopoiesis after 5-FU and cisplatin injury

To determine whether D1R could accelerate hematopoietic reconstitution regardless of the cytotoxic agent, C57BL/6 mice were injected once daily for 7 days with 5-fluorouracil (5-FU) or cisplatin and then injected with D1R or PBS 2 h later. Likewise, D1R-treated mice displayed better hematopoietic regeneration than mice receiving PBS both in 5-FU- and cisplatin-chemotherapeutic mice (**Figure 5A** and **5B**). Moreover, consistent with the primary increase of the myeloid lineage in multi-lineage contribution (**Figures 5C**, **5D**, S4A and S4B), greater numbers of LSK cells in spleen (**Figure 5E** and **5F**) and $Lin^-Sca\text{-}1^-c\text{-}Kit^+$ cells in BM (**Figure 5E**) were observed in D1R-treated mice, representing functional HSCs and myeloid progenitor cells, respectively. There were also an expanded number of B cells in D1R-treated mice compared to PBS-treated mice (Figure S4C and S4D). Overall, we further validated Notch signaling as a potential countermeasure to stimulate HSC regeneration following myelotoxic stress.

Notch signaling promotes HSC proliferation by modulating the PI3K/ERK/BAD signaling axis following stress

Given the profound elevation of HSCs, we sought to determine whether Notch activation

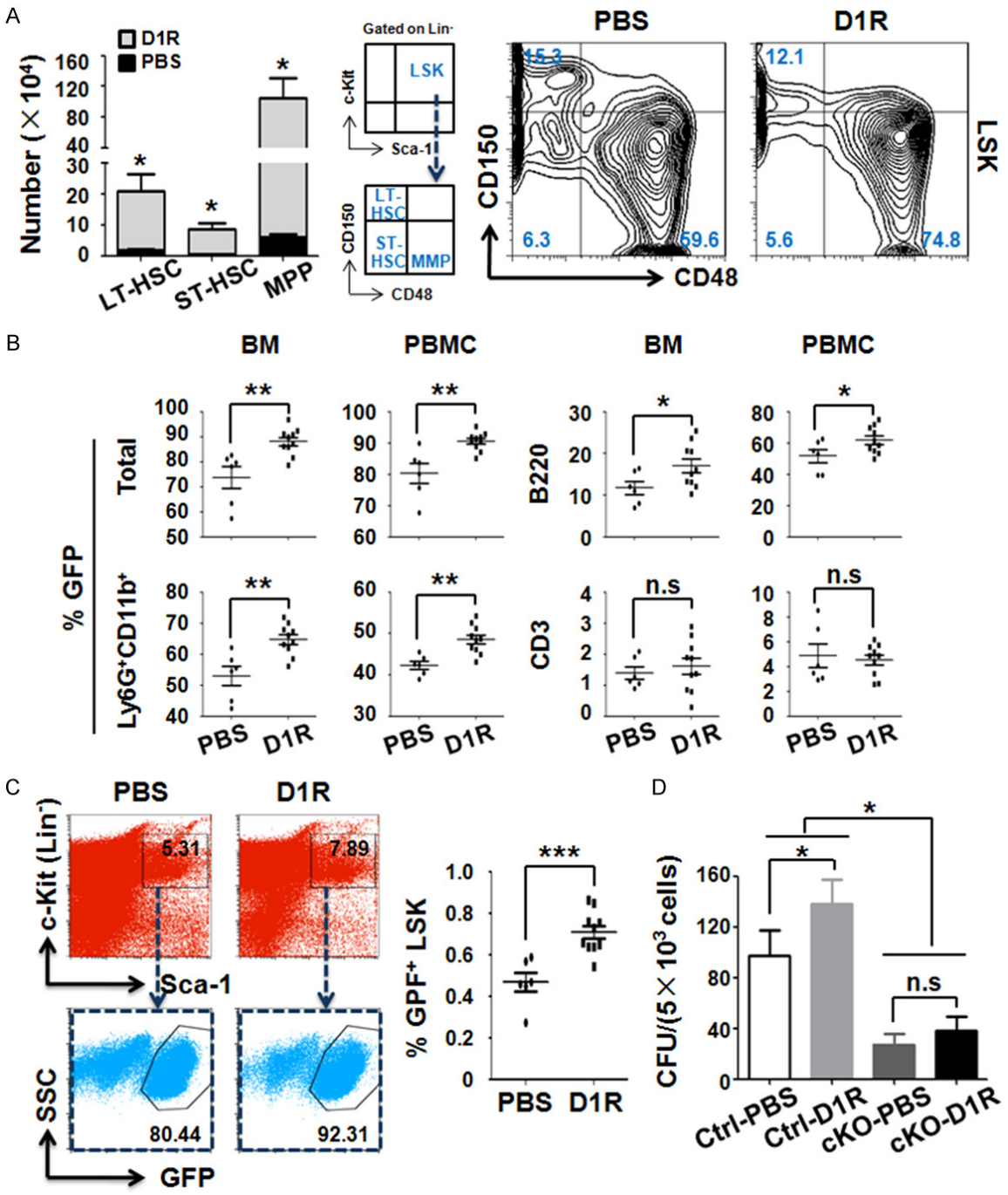

Figure 4. Notch signaling improves HSC regeneration following CTX. A. Total numbers (left) and representative FACS plots (right) of long-term HSC (LT-HSC), short-term HSC (ST-HSC) and multipotent progenitor (MPP) in PBS- or D1R-treated mice 7 day after CTX chemotherapy. B. BM and PBMCs GFP$^+$ engraftment percentages of total nucleated cells, myeloid (Ly6G$^+$CD11b$^+$), B-cell (B220$^+$) and T-cell (CD3$^+$) at 8 weeks following competitive bone marrow transplantation. C. Representative plots (left) and percentage (right) of donor GFP$^+$ cells within the LSK population at 8 weeks after transplantation. D. Total CFU colonies of BM cells in Mx1-Cre-RBP-J$^{f/f}$ (cKO) and Mx1-Cre-RBP-J$^{f/+}$ (Ctrl) mice which were daily injected with D1R or PBS for 7 days after 150 mg/kg CTX treatment. Data are presented as the means ± SEM (n=8). *P < 0.05, **P < 0.01, ***P < 0.01 vs PBS.

would promote HSC proliferation. A bromodeoxyuridine incorporation assay revealed increased proportions of proliferating LSK cells (**Figure 6A**) and myeloid precursor cells (Figure

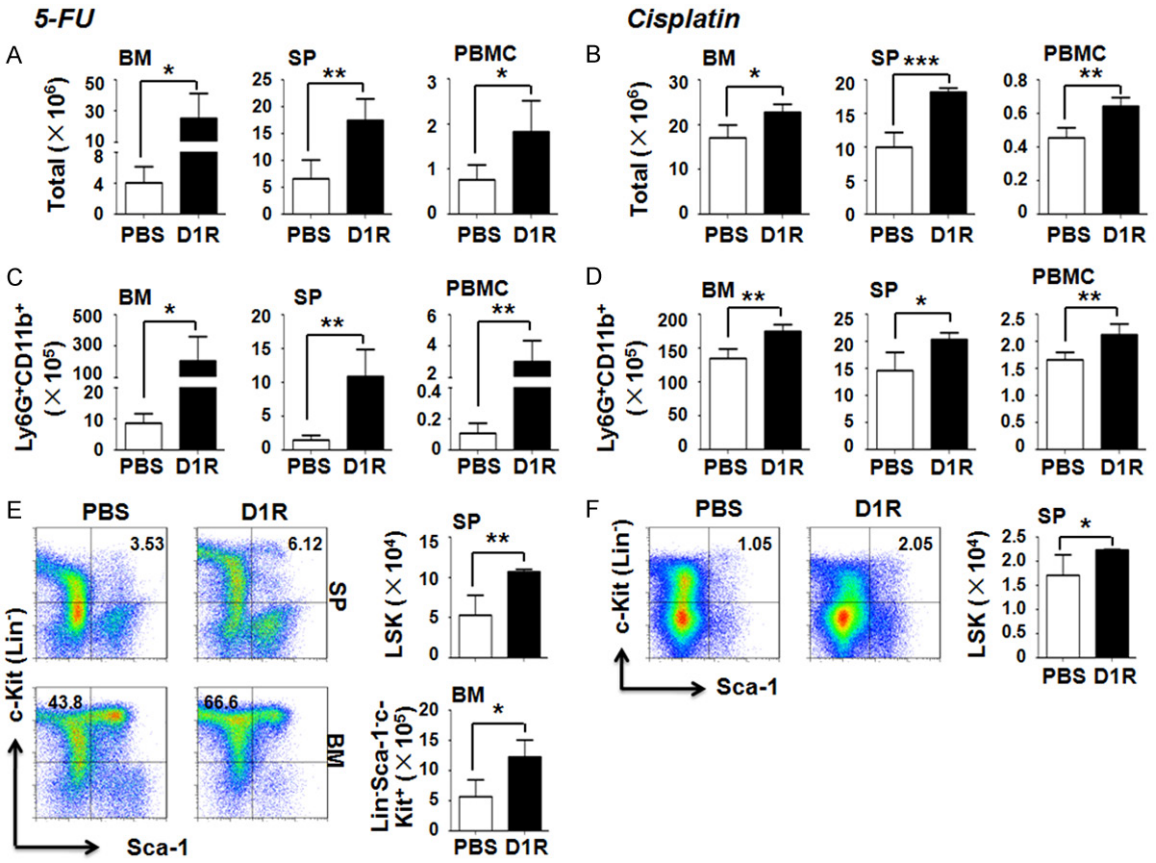

Figure 5. Notch signaling restores hematopoiesis after 5-FU and cisplatin injury. 8-week-old C57BL/6 mice were intraperitoneally injected with PBS or D1R daily for 7 days post 5-FU (150 mg/kg) or cisplatin (5 mg/kg) chemotherapy. (A, B) BM, spleen and PBMCs of PBS or D1R treated mice after 5-FU (A) or cisplatin (B) administration. (C, D) Marrow, spleen and blood myeloid cells ($Ly6G^+CD11b^+$) from PBS- or D1R-treated mice following 5-FU (C) or cisplatin (D). (E) Representative flow cytometric analysis (left) and total numbers (right) of LSK cells and myeloid progenitor ($Lin^-Sca\text{-}1^-c\text{-}Kit^+$) in marrow and spleen after 5-FU. (F) Representative plots (left) and numbers (right) of spleen LSK cells following cisplatin. Data are presented as the means ± SEM (n=6). $^*P < 0.05$, $^{**}P < 0.01$, $^{***}P < 0.001$ vs PBS.

S5A) in BM from D1R-treated mice 7 days after CTX exposure. Consistent with these results, we found a higher proportion of LSK cells in the S phase and a decreased proportion in the G_0/G_1 phase were detected in D1R-injected chemotherapeutic mice in comparison to PBS-treated mice (**Figure 6B**). Additionally, the apoptosis analysis revealed no statistical difference in live, apoptotic, and dead cells between D1R- and PBS-treated mice (Figure S5B). Mechanistically, Notch activation maintained HSCs in a brief and transient proliferative period to accelerate hematopoietic reconstruction rapidly after chemical-induced myelosuppression.

To further confirm this hypothesis, we evaluated the key molecules associated with HSC self-renewal, proliferation, cycling, apoptosis, and quiescence. Within these categories, D1R treatment dramatically upregulated phosphorylation of ERK1/2 and PI3K *in vivo*, corresponding to repression of the apoptotic genes BAD and Bcl-2-associated X (BAX) as well as an increase of the anti-apoptotic gene BCL2 following CTX (**Figure 6C**). Further, transcriptome analysis of Cyclin D1 (Ccnd1), identified to be critical in the cell cycle, was enriched in LSK cells from D1R-treated mice (**Figure 6D**). Consistent with our previous finding [7], Csf1, Csf2r, and Csf2rb2 increased in LSK cells purified from D1R-treated mice. All these markers are related to myelopoiesis (**Figure 6D**). These findings indicate that Notch signaling mediated HSC proliferation partially through the PI3K/ERK/BAD signaling axis in response to a myelosuppressive stressor.

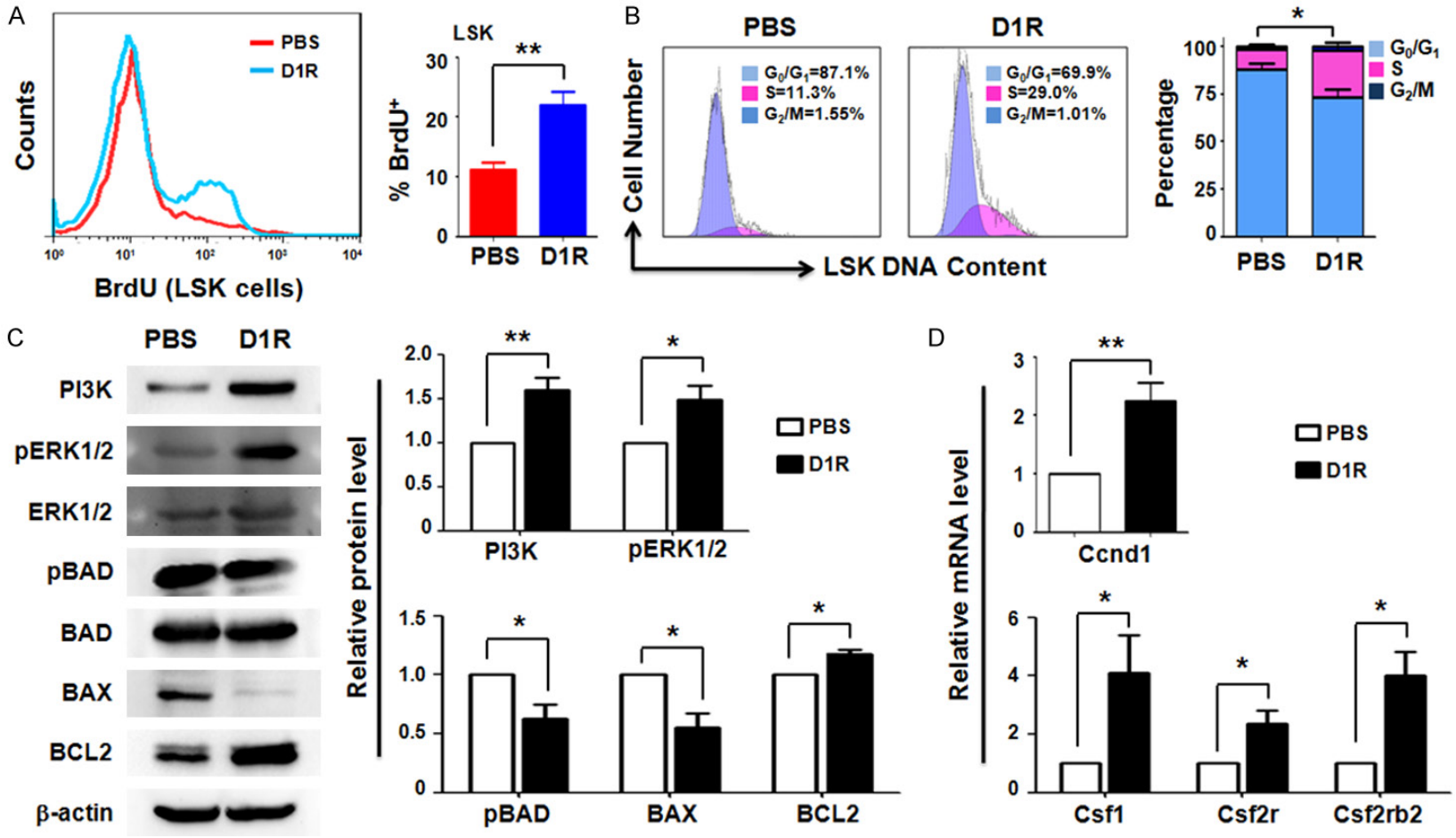

Figure 6. Notch signaling promotes HSCs proliferation by modulating PI3K/ERK/BAD signaling axis following stress. 8-week-old C57BL/6 mice were daily injected with PBS or D1R for 7 days after CTX exposure. A. Representative FACS profiles (left) and percentages (right) of BrdU-retaining LSK cells in BM. B. Representative FACS plots (left) and frequencies (right) of BM LSK cells in phases of cell cycle. C. Western blot images (left) and relative quantification (right) of PI3K, Erk1/2, pErk1/2, Bad, pBad, Bax, Bcl-2 and β-actin in sorted BM LSK cells. D. Ccnd1, Csf1, Csf2r and Csf2rb2 mRNA expression in LSK fractions by qRT-PCR. Data are presented as the means ± SEM (n=6). $*P < 0.05$, $**P < 0.01$ vs PBS.

Notch signaling induces c-Myc expression to improve hematopoietic repopulation

To further understand the key molecular effect of Notch stimulation in HSC proliferation after chemotherapy-induced myeloablation, we analyzed our previous gene database derived from D1R-expanded HSCs [8] and found a significant elevation of c-Myc, which was previously identified as critical in HSC proliferation, differentiation, and survival [12]. Notch activation increased the c-Myc transcription in LSK cells in D1R-treated chemotherapeutic mice (**Figure 7A**). Meanwhile, the expression of c-Myc was significantly reduced in LSK fractions from RBP-J knockdown mice after CTX challenge (**Figure 7B**). A strong overlap of an RBP-J-binding site (TGGGAA) on the promoter of c-Myc was identified using an existing in silico analysis of a chromatin immunoprecipitation followed by a sequencing dataset (Figure S6A) [13]. We therefore hypothesized that D1R-mediated c-Myc activation could benefit HSC proliferation after myelotoxic stress.

To test this hypothesis *in vivo*, we created hematopoietic chimeras by implanting LSK cells stably expressing Ctrl-shRNA-EGFP (shCtrl) or c-Myc-shRNA-EGFP (shc-Myc) (Figure S6B). These donor cells were mixed with congenic competing BM cells and transplanted into lethally irradiated C57BL/6 recipient mice. We exposed chimeric mice to CTX 8 weeks post-transplantation and subsequently administered D1R or PBS for 7 days (Figure S6C). Constitutive abrogation of c-Myc resulted in a significant reduction in survival (**Figure 7C**) and multi-lineage hematopoietic reconstitution in peripheral blood (**Figures 7D** and S6D), as well as an increase in LSK percentage (**Figure 7E**). As expected, D1R treatment caused increased LSK, myeloid, and B cells engraftment compared to PBS treatment in lentivirus control mice, which were not rescued by D1R in c-Myc knockdown mice (**Figures 7D**, **7E** and S6D). Consistent with our hypothesis, D1R-treated recipients had decreased EGFP chimerism in comparison to PBS-treated recipients (**Figures 7F**, **7G** and S6D), which was relevant to the asymmetric increase of both EGFP negative and positive chimeric donor LSK compartments in c-Myc-ablated recipient animals (**Figure 7E**). These results collectively indicated that Notch signaling mitigated chemotherapy toxicity partially dependent on c-Myc-induced hematopoietic cell proliferation.

Discussion

BM toxicity is a common dose-limiting side-effect for malignant tumor patients undergoing chemoradiotherapy, immune-checkpoint therapy, and molecular-targeted therapy. Available approaches to facilitate hematopoietic recovery are still limited. HSCs, the core of hematopoietic recovery, reside in the BM specialized micro-anatomical environment. The perivascular niche predominantly regulates HSC homeostatic balance among quiescence, self-renewal, and differentiation through multiple factors, such as signaling lymphocytic activation molecule, stem cell factor, C-C motif chemokine ligand 12, membrane-bound stem cell factor, thrombopoietin, angiopoietin-1, transforming growth factor-β, and the Notch pathway [14-16].

Notch signaling is thought to determine the cell fate of HSCs, neural stem cells, and muscle stem cells, as well as the development of T cells and vessels [17-19]. Recent studies show that Notch can be both tumor suppressive and oncogenic in T cell acute lymphoblastic leukemia, acute myeloid leukemia, and small-cell lung cancer [20, 21]. Previous studies suggest the Notch pathway is an HSC-expander and a radio-protector depending on the context [7, 8, 22]. Nonetheless, its role in mitigating chemotherapeutic cytotoxin *in vivo* remains unknown. Because the mechanisms driving hematopoietic reconstruction are not directly transposable between irradiation and chemotherapy [23, 24], we sought to address these differences.

Here, we revealed that blocking Notch signaling in inducible genetic mice impaired hematopoiesis regeneration after myelosuppressive chemotherapy. Complementarily, spatiotemporally constrained activation of Notch signaling through pharmacologic gain-of-function mice accelerated multi-lineage hematopoietic reconstitution after treatment with various cytotoxins. Moreover, both LT-HSC and ST-HSC contents were preferentially repopulated in a Notch-dependent manner after hematopoietic insult. Compatible with our murine experimental observations, clinical association substantiated that allo-HCT patients with GGF displayed a

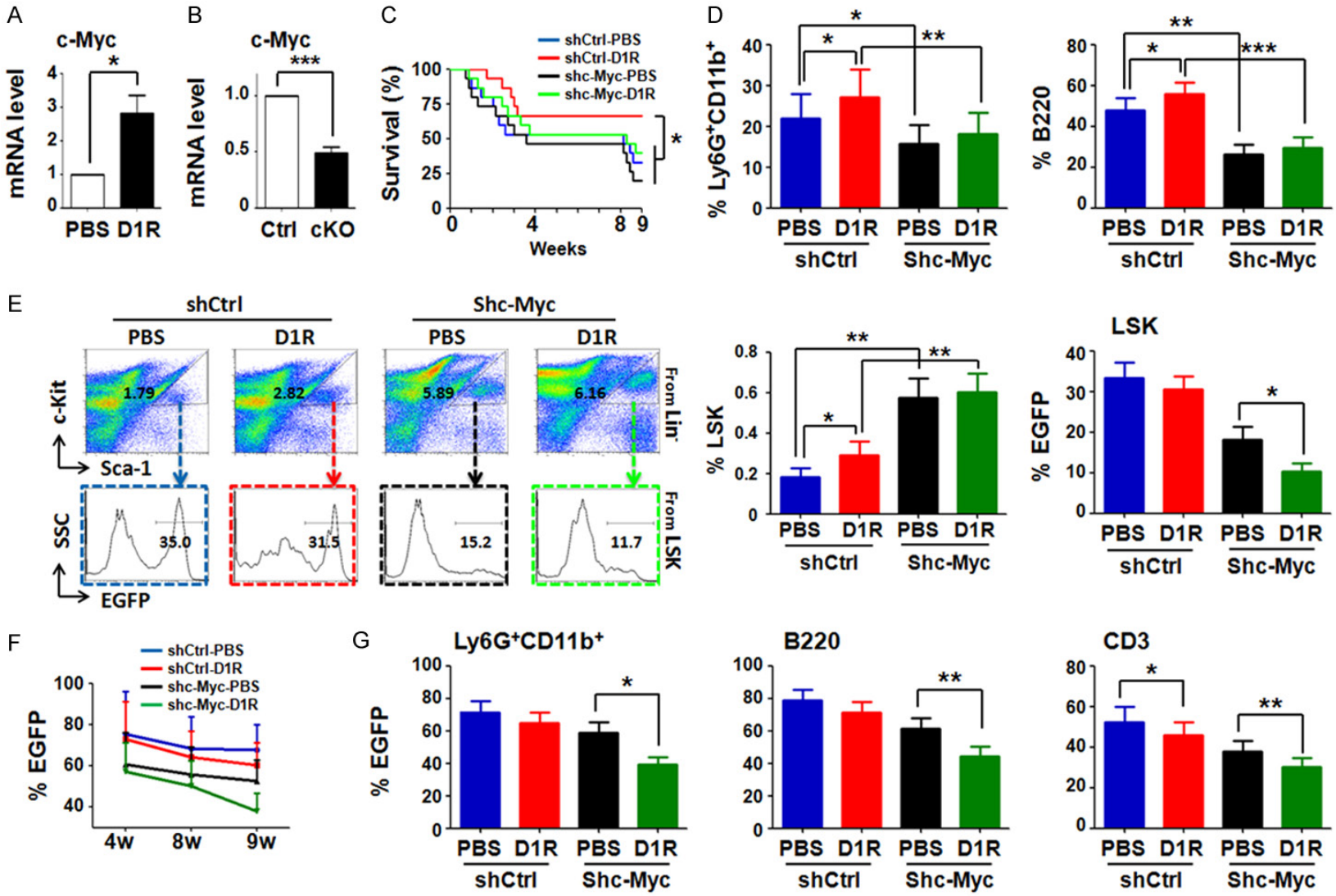

Figure 7. Notch signaling induces c-Myc expression to improve hematopoietic repopulation. (A, B) Expression of c-Myc in BM LSK cells isolated from PBS- or D1R-treated C57BL/6 mice (A), as well as from Mx1-Cre-RBP-J$^{f/f}$ (cKO) or Mx1-Cre-RBP-J$^{f/+}$ (Ctrl) mice (B) at day 7 following CTX challenge. (C-G) Ctrl-shRNA-EGFP (shCtrl) or c-Myc-shRNA-EGFP (shc-Myc) transfected LSK cells (5 × 10^3) mixed with BM cells (5 × 10^5) from C57BL/6 mice, were transplanted to C57BL/6 recipient mice through tail vein injection after 1000 cGy lethal TBI. The chimeric mice were daily treated with D1R or PBS for 7 days following CTX exposure at 8-weeks post-transplantation. (C) Survival curve. (D) Percentages of myeloid (Ly6G$^+$CD11b$^+$) and B-cell (B220$^+$) in PBMCs at 9 weeks after HSCT. (E) Representative flow cytometric analysis (left), percentages of LSK

engraftment (middle) and EGFP$^+$ LSK engraftment (right) in BM at 9-weeks post-transplantation. (F) PBMCs EGFP$^+$ engraftment at 4-, 8- and 9-weeks post-transplantation. (G) PBMCs EGFP$^+$ engraftment of myeloid-, T- and B-cells. Data are presented as the means ± SEM (n=6). *P < 0.05, **P < 0.01, ***P < 0.001 vs Ctrl or vs PBS.

high level of Notch activation and vice versa. These results provide evidence that the Notch pathway could be an effective strategy to limit myelosuppression from chemotherapy.

The endothelial-targeted Notch recombinant ligand protein D1R might also activate Notch signaling in the vascular niche microenvironment, especially in ECs, which are essential for the self-renewal and repopulation of Notch-dependent HSCs [25]. Therefore, it is important to investigate whether the positive role of D1R in the current study is mediated through HSPC-specific Notch activation. We induced a D1R-induced Notch signaling activation in BM HSPCs *in vivo*. Furthermore, D1R promoted hematopoietic recovery in wild-type, but not RBP-J-deficient mice. As such, this finding indicates that D1R partially modulates hematopoietic regeneration in a HSPC-specific, Notch-dependent manner.

We further demonstrated that Notch mitigated chemotoxicity was not mediated by attenuating apoptosis, but rather due to transiently switching HSCs to a proliferative state, which is inconsistent with our previous study [7]. A possible explanation for this discrepancy is that D1R-mediated signaling has distinct spatiotemporal effects on HSCs in response to cytotoxicity versus irradiation, due to the different mechanisms by which they cause damage. Ionizing radiation primarily induces acute hematopoietic toxicity, such as HSC apoptosis and senescence [26]. However, cytotoxic drugs cause long-term hematopoietic exhaustion by dose-limiting late myelotoxicity to HSCs [27, 28]. In this work, transient and reversible proliferation is critical to attenuate chemotherapy-induced HSC exhaustion and to adequately meet increased hematopoietic demands. The subsequently reduced proliferative burden can protect quiescent HSCs to avoid hematopoietic exhaustion and to maintain long-term hematopoiesis. We therefore sought to address the specific mechanism of Notch-induced HSC proliferation at the time of exposure to cytotoxic agents.

HSC activation is driven in part through interferon-α, interferon-γ, granulocyte colony-stimulating factor, and ERK signaling [29, 30]. However, the relationship between Notch and HSC proliferation remains poorly understood. Our data showed that Notch ingeniously drives a harmonious signaling network in parallel with an upregulated PI3K/ERK proliferation pathway, elevated BCL2 survival signaling, downregulated BAD/BAX apoptosis axis, as well as overexpressed Ccnd1 for G_0/G_1-S transition. Several lines of evidence point to a link between PI3K/AKT/mTORC1 signaling and HSC activation, but some studies delineate that HSC dormancy is mediated partly through the ERK pathway [29, 31]. In the current study, we detected a Notch-mediated synchronous upregulation of PI3K-ERK signaling in HSCs during a cytotoxic emergency. We propose that key molecules could contribute to Notch-induced HSC recovery in chemotherapeutic emergency hematopoiesis.

Our data describe a Notch-modulated critical role of c-Myc in maintaining HSC viability during metabolically unfavorable conditions. Previous research has shown that Myc precisely regulates normal HSC hierarchies including self-renewal, proliferation, differentiation, and survival by highly-combinatorial enhancer systems [12, 32]. Partial knockdown of c-Myc by lentivirus results in severe cytopenia and accumulation of ineffective HSCs in situ, supporting previous observations that conditional elimination of c-Myc in the BM results in mutant HSC failure to initiate normal stem cell differentiation [33]. Nevertheless, Myc controls the biosynthetic machinery of stem cells without affecting their potency [34]. Thus, activation of Notch signaling *in vivo* shows beneficial effects on multi-lineage reconstitution; although, D1R-treated recipient mice displayed decreased EFGP donor engraftment. This inconsistency might be a response to the different reconstruction efficiencies of EGFP positive and negative donor cells in chimeric recipients. In addition, we previously confirmed the safety of Notch activation through *in vivo* competitive repopulation conditions [7]. Further investigations are required to elucidate the relationship between c-Myc and the PI3K/ERK axis in hematopoietic reconstitution dominated by the Notch pathway.

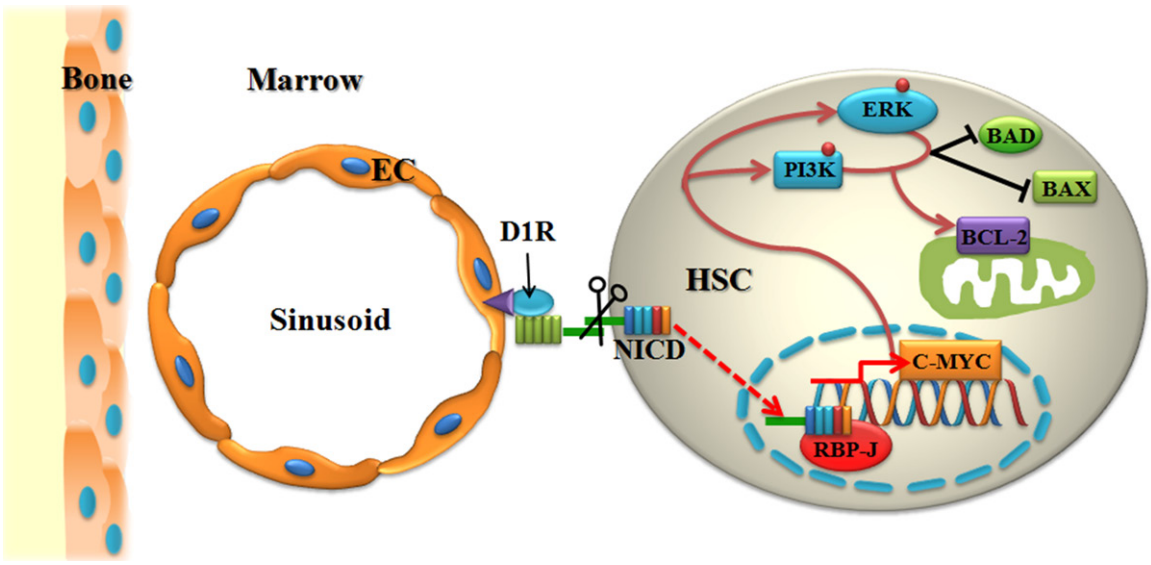

Figure 8. Graphic illustration of the study. D1R mediates Notch activation in a EC-HSC manner, and promotes multi-lineage hematopoietic reconstitution from chemotherapy-induced exhaustion by transiently accelerating HSCs proliferation partially via c-Myc.

We also observed moderate Notch-related myeloid skewing following chemotherapeutics myelosuppression, partially consistent with our previous study [7]. A recent study suggested that Notch is dispensable for myeloid progenitors in adult steady-state RBP-J deficient mice [35]; however, it has also been reported that Notch signaling distinctly contributes to myeloid differentiation through cell-cell contact-dependent mechanisms in normal and stress hematopoiesis, including upstream signaling of bone morphogenetic protein [36], a disintegrin and metalloproteinase 10 [37], and nuclear factor erythroid-2-related factor 2 [38], as well as downstream signaling of nuclear factor kappa B, PU.1, CCAAT/enhancer binding protein α, and interleukin-6 [39]. These factors were also implicated in acute megakaryoblastic leukemia and myeloid malignancies [40, 41]. Consequently, the controversial role of canonical Notch signaling in myeloid differentiation is context-dependent and remains to be defined.

Conclusions

In conclusion, the present study demonstrated a previously unrecognized role for Notch signaling in the regulation of HSC regeneration after myelosuppressive chemotherapy. Notch activation resulted in efficient and transient HSC proliferation and expansion, which correlated with activation of the downstream PI3K/ERK/BAD signaling axis, which was at least partially due to the upregulation of c-Myc (**Figure 8**). Unlike lineage-specific strategies such as transfusions and hematopoietic growth factors, endothelial-targeted Notch pharmacologic gain-of-function was multi-lineage comprehensive, sustainable, and safe. Therefore, our work here emphasizes the prominent role of Notch signaling in ameliorating short- and long-term myelosuppressive injury after cytotoxic agents, demonstrating therapeutic potential for preclinical translation.

Acknowledgements

We are grateful to Hua Han and Yingming Liang for providing expert technical assistance. This work was supported by grants from the Natural Science Foundation of Guangdong Province (2018A030313571, 2017A030310649).

Disclosure of conflict of interest

None.

Abbreviations

allo-HCT, allogeneic hematopoietic stem cells transplantation; BM, bone marrow; BrdU, 5-bromo-2'-deoxyuridine; CMP, common myeloid progenitors; CTX, cyclophosphamide; DSL, Delta-Serrate-Lag-2; ECs, endothelial cells; FACS, fluorescence-activated cell sorting; GGF, good

graft function; GMP, granulocyte/monocyte progenitors; HSCs, hematopoietic stem cells; HSCT, hematopoietic stem cells transplantation; HSPCs, hematopoietic stem/progenitor cells; ICN1, intracellular domains of Notch 1; LT-HSCs, long-term hematopoietic stem cells; MEP, myeloid/erythroid progenitors; MPP, multipotent progenitor; NICD, Notch intracellular domain; PBMC, peripheral blood mononuclear cells; PBS, phosphate-buffered saline; PGF, poor graft function; RBP-J, recombination signal binding protein Jκ; RGD, arginine-glycine-aspartic acid; ST-HSCs, short-term hematopoietic stem cells; 5-FU, 5-fluorouracil.

Address correspondence to: Dr. Juanjuan Chen, State Key Laboratory of Organ Failure Research, Guangdong Provincial Key Laboratory of Viral Hepatitis Research, Department of Infectious Diseases, Nanfang Hospital, Southern Medical University, 1838 Guangzhou Avenue North, Guangzhou 510515, Guangdong, China. Tel: +86-20-62786539; Fax: +86-20-62787428; E-mail: chenjj@smu.edu.cn

References

[1] Zhao K and Liu Q. The clinical application of mesenchymal stromal cells in hematopoietic stem cell transplantation. J Hematol Oncol 2016; 9: 46.

[2] Pinho S and Frenette PS. Haematopoietic stem cell activity and interactions with the niche. Nat Rev Mol Cell Biol 2019; 20: 303-320.

[3] Blaser BW and Zon LI. Making HSCs in vitro: don't forget the hemogenic endothelium. Blood 2018; 132: 1372-1378.

[4] Itkin T, Gur-Cohen S, Spencer JA, Schajnovitz A, Ramasamy SK, Kusumbe AP, Ledergor G, Jung Y, Milo I, Poulos MG, Kalinkovich A, Ludin A, Kollet O, Shakhar G, Butler JM, Rafii S, Adams RH, Scadden DT, Lin CP and Lapidot T. Distinct bone marrow blood vessels differentially regulate haematopoiesis. Nature 2016; 532: 323-328.

[5] Guo P, Poulos MG, Palikuqi B, Badwe CR, Lis R, Kunar B, Ding B, Rabbany SY, Shido K, Butler JM and Rafii S. Endothelial jagged-2 sustains hematopoietic stem and progenitor reconstitution after myelosuppression. J Clin Invest 2017; 127: 4242-4256.

[6] Kusumbe AP, Ramasamy SK, Itkin T, Mäe MA, Langen UH, Betsholtz C, Lapidot T and Adams RH. Age-dependent modulation of vascular niches for haematopoietic stem cells. Nature 2016; 532: 380-384.

[7] Chen JJ, Gao XT, Yang L, Fu W, Liang L, Li JC, Hu B, Sun ZJ, Huang SY, Zhang YZ, Liang YM, Qin HY and Han H. Disruption of Notch signaling aggravates irradiation-induced bone marrow injury, which is ameliorated by a soluble Dll1 ligand through Csf2rb2 upregulation. Sci Rep 2016; 6: 26003.

[8] Tian DM, Liang L, Zhao XC, Zheng MH, Cao XL, Qin HY, Wang CM, Liang YM and Han H. Endothelium-targeted Delta-like 1 promotes hematopoietic stem cell expansion ex vivo and engraftment in hematopoietic tissues in vivo. Stem Cell Res 2013; 11: 693-706.

[9] Han H, Tanigaki K, Yamamoto N, Kuroda K, Yoshimoto M, Nakahata T, Ikuta K and Honjo T. Inducible gene knockout of transcription factor recombination signal binding protein-J reveals its essential role in T versus B lineage decision. Int Immunol 2002; 14: 637-645.

[10] Shukla S, Langley MA, Singh J, Edgar JM, Mohtashami M, Zúñiga-Pflücker JC and Zandstra PW. Progenitor T-cell differentiation from hematopoietic stem cells using Delta-like-4 and VCAM-1. Nat Methods 2017; 14: 531-538.

[11] Chang YJ, Zhao XY, Xu LP, Zhang XH, Wang Y, Han W, Chen H, Wang FR, Mo XD, Zhang YY, Huo MR, Zhao XS, Y K, Liu KY and Huang XJ. Donor-specific anti-human leukocyte antigen antibodies were associated with primary graft failure after unmanipulated haploidentical blood and marrow transplantation: a prospective study with randomly assigned training and validation sets. J Hematol Oncol 2015; 8: 84.

[12] Hishida T, Nakachi Y, Mizuno Y, Katano M, Okazaki Y, Ema M, Takahashi S, Hirasaki M, Suzuki A, Ueda A, Nishimoto M, Hishida-Nozaki Y, Vazquez-Ferrer E, Sancho-Martinez I, Belmonte JC and Okuda A. Functional compensation between Myc and PI3K signaling supports self-renewal of embryonic stem cells. Stem Cells 2015; 33: 713-725.

[13] Dasgupta S, Rajapakshe K, Zhu B, Nikolai BC, Yi P, Putluri N, Choi JM, Jung SY, Coarfa C, Westbrook TF, Zhang XH, Foulds CE, Tsai SY, Tsai MJ and O'Malley BW. Metabolic enzyme PFKFB4 activates transcriptional coactivator SRC-3 to drive breast cancer. Nature 2018; 556: 249-254.

[14] Ehninger A, Boch T, Medyouf H, Müdder K, Orend G and Trumpp A. Loss of SPARC protects hematopoietic stem cells from chemotherapy toxicity by accelerating their return to quiescence. Blood 2014; 123: 4054-4063.

[15] Zhao M, Perry JM, Marshall H, Venkatraman A, Qian P, He XC, Ahamed J and Li L. Megakaryocytes maintain homeostatic quiescence and promote post-injury regeneration of hematopoietic stem cells. Nat Med 2014; 20: 1321-1326.

[16] Morrison SJ and Scadden DT. The bone marrow niche for haematopoietic stem cells. Nature 2014; 505: 327-334.

[17] Polacheck WJ, Kutys ML, Yang J, Eyckmans J, Wu Y, Vasavada H, Hirschi KK and Chen CS. A non-canonical Notch complex regulates adherens junctions and vascular barrier function. Nature 2017; 552: 258-262.
[18] Liu L, Charville GW, Cheung TH, Yoo B, Santos PJ, Schroeder M and Rando TA. Impaired Notch signaling leads to a decrease in p53 activity and mitotic catastrophe in aged muscle stem cells. Cell Stem Cell 2018; 23: 544-556.
[19] Huang B, Wang Y, Wang W, Chen J, Lai P, Liu Z, Yan B, Xu S, Zhang Z, Zeng C, Rong L, Liu B, Cai D, Jin D and Bai X. mTORC1 prevents preosteoblast differentiation through the Notch signaling pathway. PLoS Genet 2015; 11: e1005426.
[20] Lim JS, Ibaseta A, Fischer MM, Cancilla B, O'Young G, Cristea S, Luca VC, Yang D, Jahchan NS, Hamard C, Antoine M, Wislez M, Kong C, Cain J, Liu YW, Kapoun AM, Garcia KC, Hoey T, Murriel CL and Sage J. Intratumoural heterogeneity generated by Notch signalling promotes small-cell lung cancer. Nature 2017; 545: 360-364.
[21] Sanchez-Martin M, Ambesi-Impiombato A, Qin Y, Herranz D, Bansal M, Girardi T, Paietta E, Tallman MS, Rowe JM, De Keersmaecker K, Califano A and Ferrando AA. Synergistic anti-leukemic therapies in NOTCH 1-induced T-ALL. Proc Natl Acad Sci U S A 2017; 114: 2006-2011.
[22] Delaney C, Heimfeld S, Brashem-Stein C, Voorhies H, Manger RL and Bernstein ID. Notch-mediated expansion of human cord blood progenitor cells capable of rapid myeloid reconstitution. Nat Med 2010; 16: 232-236.
[23] Insinga A, Cicalese A, Faretta M, Gallo B, Albano L, Ronzoni S, Furia L, Viale A and Pelicci PG. DNA damage in stem cells activates p21, inhibits p53, and induces symmetric self-renewing divisions. Proc Natl Acad Sci U S A 2013; 110: 3931-3936.
[24] Mandal PK and Rossi DJ. DNA-damage-induced differentiation in hematopoietic stem cells. Cell 2012; 148: 847-848.
[25] Butler JM, Nolan DJ, Vertes EL, Varnum-Finney B, Kobayashi H, Hooper AT, Seandel M, Shido K, White IA, Kobayashi M, Witte L, May C, Shawber C, Kimura Y, Kitajewski J, Rosenwaks Z, Bernstein ID and Rafii S. Endothelial cells are essential for the self-renewal and repopulation of Notch-dependent hematopoietic stem cells. Cell Stem Cell 2010; 6: 251-264.
[26] Himburg HA, Doan PL, Quarmyne M, Yan X, Sasine J, Zhao L, Hancock GV, Kan J, Pohl KA, Tran E, Chao NJ, Harris JR and Chute JP. Dickkopf-1 promotes hematopoietic regeneration via direct and niche-mediated mechanisms. Nat Med 2017; 23: 91-99.
[27] He S, Roberts PJ, Sorrentino JA, Bisi JE, Storrie-White H, Tiessen RG, Makhuli KM, Wargin WA, Tadema H, van Hoogdalem EJ, Strum JC, Malik R and Sharpless NE. Transient CDK4/6 inhibition protects hematopoietic stem cells from chemotherapy-induced exhaustion. Sci Transl Med 2017; 9: eaal3986.
[28] Piryani SO, Kam AYF, Kliassov EG, Chen BJ, Spector NL, Chute JP, Hsu DS, Chao NJ and Doan PL. Epidermal growth factor and granulocyte colony stimulating factor signaling are synergistic for hematopoietic regeneration. Stem Cells 2018; 36: 252-264.
[29] Baumgartner C, Toifl S, Farlik M, Halbritter F, Scheicher R, Fischer I, Sexl V, Bock C and Baccarini M. An ERK-dependent feedback mechanism prevents hematopoietic stem cell exhaustion. Cell Stem Cell 2018; 22: 879-892.
[30] Baldridge MT, King KY, Boles NC, Weksberg DC and Goodell MA. Quiescent haematopoietic stem cells are activated by IFN-gamma in response to chronic infection. Nature 2010; 465: 793-797.
[31] Rodgers JT, King KY, Brett JO, Cromie MJ, Charville GW, Maguire KK, Brunson C, Mastey N, Liu L, Tsai CR, Goodell MA and Rando TA. mTORC1 controls the adaptive transition of quiescent stem cells from G0 to G(Alert). Nature 2014; 510: 393-396.
[32] Bahr C, von Paleske L, Uslu VV, Remeseiro S, Takayama N, Ng SW, Murison A, Langenfeld K, Petretich M, Scognamiglio R, Zeisberger P, Benk AS, Amit I, Zandstra PW, Lupien M, Dick JE, Trumpp A and Spitz F. A Myc enhancer cluster regulates normal and leukaemic haematopoietic stem cell hierarchies. Nature 2018; 553: 515-520.
[33] Wilson A, Murphy MJ, Oskarsson T, Kaloulis K, Bettess MD, Oser GM, Pasche AC, Knabenhans C, Macdonald HR and Trumpp A. c-Myc controls the balance between hematopoietic stem cell self-renewal and differentiation. Genes Dev 2004; 18: 2747-2763.
[34] Scognamiglio R, Cabezas-Wallscheid N, Thier MC, Altamura S, Reyes A, Prendergast ÁM, Baumgärtner D, Carnevalli LS, Atzberger A, Haas S, von Paleske L, Boroviak T, Wörsdörfer P, Essers MA, Kloz U, Eisenman RN, Edenhofer F, Bertone P, Huber W, van der Hoeven F, Smith A and Trumpp A. Myc depletion induces a pluripotent dormant state mimicking diapause. Cell 2016; 164: 668-680.
[35] Duarte S, Woll PS, Buza-Vidas N, Chin DWL, Boukarabila H, Luís TC, Stenson L, Bouriez-Jones T, Ferry H, Mead AJ, Atkinson D, Jin S, Clark SA, Wu B, Repapi E, Gray N, Taylor S, Mutvei AP, Tsoi YL, Nerlov C, Lendahl U and Jacobsen SEW. Canonical Notch signaling is dispensable for adult steady-state and stress

myelo-erythropoiesis. Blood 2018; 131: 1712-1719.
[36] Cook BD and Evans T. BMP signaling balances murine myeloid potential through SMAD-independent p38MAPK and NOTCH pathways. Blood 2014; 124: 393-402.
[37] Gibb DR, Saleem SJ, Kang DJ, Subler MA and Conrad DH. ADAM10 overexpression shifts lympho- and myelopoiesis by dysregulating site 2/site 3 cleavage products of Notch. J Immunol 2011; 186: 4244-4252.
[38] Kim JH, Thimmulappa RK, Kumar V, Cui W, Kumar S, Kombairaju P, Zhang H, Margolick J, Matsui W, Macvittie T, Malhotra SV and Biswal S. NRF2-mediated Notch pathway activation enhances hematopoietic reconstitution following myelosuppressive radiation. J Clin Invest 2014; 124: 730-741.
[39] Csaszar E, Wang W, Usenko T, Qiao W, Delaney C, Bernstein ID and Zandstra PW. Blood stem cell fate regulation by Delta-1-mediated rewiring of IL-6 paracrine signaling. Blood 2014; 123: 650-658.
[40] Bill M, Pathmanathan A, Karunasiri M, Shen C, Burke MH, Ranganathan P, Papaioannou D, Zitzer NC, Snyder K, LaRocco A, Walker AE, Brannan ZJ, Nalin AP, Freud AG, Dikov MM, Zhang X, Bloomfield CD, Garzon R and Dorrance AM. EGFL7 antagonizes NOTCH signaling and represents a novel therapeutic target in acute myeloid leukemia. Clin Cancer Res 2020; 26: 669-678.
[41] Xiu Y, Dong Q, Fu L, Bossler A, Tang X, Boyce B, Borcherding N, Leidinger M, Sardina JL, Xue HH, Li Q, Feldman A, Aifantis I, Boccalatte F, Wang L, Jin M, Khoury J, Wang W, Hu S, Yuan Y, Wang E, Yuan J, Janz S, Colgan J, Habelhah H, Waldschmidt T, Müschen M, Bagg A, Darbro B and Zhao C. Coactivation of NF-κB and Notch signaling is sufficient to induce B cell transformation and enables B-myeloid conversion. Blood 2020; 135: 108-120.

Table S1. Antibodies used in this study

Name	Supplier	Clone #
anti-mouse BrdU-APC	eBioscience	Bu20A
anti-mouse CD34-percp/cy5.5	Biolegend	HM34
anti-mouse FcγRII/III-FITC	BD Pharmingen	2.4G2
anti-mouse CD150-percp/cy5.5	Biolegend	TC15-12F12.2
anti-mouse CD48-PE	Biolegend	HM48-1
anti-mouse CD3ε-APC	Biolegend	145-2C11
anti-mouse B220-APC	Biolegend	RA3-6B2
anti-mouse Ly6G-FITC	BD Pharmingen	1A8
anti-mouse CD11b-APC	Biolegend	M1/70
anti-mouse Sca-1-FITC	eBioscience	D7
anti-mouse c-Kit-PE	Biolegend	2B8
APC-conjugated anti-mouse lineage antibody cocktail	BD Pharmingen	145-2C11, M1/70, RA3-6B2, TER-119, Ly-76, RB6-8C5
anti-mouse Streptavidin-APC	Biolegend	polyclonal
Rabbit polyclonal to activated ICN1	Abcam	polyclonal
Cy3-conjugated goat anti-rabbit IgG	Jackson	polyclonal
ERK1/2	Cell Signaling	137F5
pERK1/2	Cell Signaling	D13.14.4E
PI3K	Cell Signaling	4249T
pBAD	Cell Signaling	5284T
BAD	Cell Signaling	9239T
BAX	Cell Signaling	Polyclonal
BCL2	Cell Signaling	D17C4
β-actin	Sigma-Aldrich	AC-15
HRP-conjugated goat anti-rabbit IgG	Boster BioTec	polyclonal
goat anti-mouse IgG	Boster BioTec	polyclonal

Table S2. Sequence of oligonucleotides and primers

Gene	Purpose	Sequence
Cre-F	Genotyping	5'-CCGGTCGATGCAACGAGTGATGAGG
Cre-R	Genotyping	5'-GCCTCCAGCTTGCATGATCTCCGG
RBP-J-F	Genotyping	5'-GTTCTTAACCTGTTGGTCGGAACC
RBP-J-WT-R	Genotyping	5'-GCTTGAGGCTTGATGTTCTGTATTGC
RBP-J-floxed-R	Genotyping	5'-ACCGGTGGATGTGGAATGTGT
β-actin-F	RT-PCR	5'-CATCCGTAAAGACCTCTATGCCAAC
β-actin-R	RT-PCR	5'-ATGGAGCCACCGATCCACA
mus Hes1-F	RT-PCR	5'-AAAGACGGCCTCTGAGCAC
mus Hes1-R	RT-PCR	5'-GGTGCTTCACAGTCATTTCCA
mus Hes5-F	RT-PCR	5'-CTGGAGATGGCCGTCAGCTA
mus Hes5-R	RT-PCR	5'-GTAGTCCTGGTGCAGGCTCTTG
mus hey1-F	RT-PCR	5'-CATGAAGAGAGCTCACCCAGA
mus hey1-R	RT-PCR	5'-CGCCGAACTCAAGTTTCC
mus hey2-F	RT-PCR	5'-GAGGAAACGACCTCCGAAA
mus hey2-R	RT-PCR	5'-GACCTCATCACTGAGCTTGTAGC
mus Delta like 1-F	RT-PCR	5'-CCCATCCGATTCCCCTTCG
mus Delta like 1-R	RT-PCR	5'-GGTTTTCTGTTGCGAGGTCATC
mus Csf2rb2-F	RT-PCR	5'-TTCCAGCCAGATCGTGACCT
mus Csf2rb2-R	RT-PCR	5'-CCCCAAGAGATACACTCCATTCC
mus Csf2r-F	RT-PCR	5'-CAATGACTACACCAACCG
mus Csf2r-R	RT-PCR	5'-GACACATCTTCTGGGCAC

mus Csf1-F	RT-PCR	5'-CGACATGGCTGGGCTCCC
mus Csf1-R	RT-PCR	5'-CGCATGGTCTCATCTATTAT
mus Ccnd1-F	RT-PCR	5'-GCGTACCCTGACACCAATCTC
mus Ccnd1-R	RT-PCR	5'-ACTTGAAGTAAGATACGGAGGGC
mus PIK3ca-F	RT-PCR	5'-CCACGACCATCTTCGGGTG
mus PIK3ca-R	RT-PCR	5'-ACGGAGGCATTCTAAAGTCACTA
mus BAX-F	RT-PCR	5'-TCGTCCATCGAGGATGACTTC
mus BAX-R	RT-PCR	5'-TGCAGAGAGAGGATACTGTAGAC
mus BCL2-F	RT-PCR	5'-ATGCCTTTGTGGAACTATATGGC
mus BCL2-R	RT-PCR	5'-GGTATGCACCCAGAGTGATGC

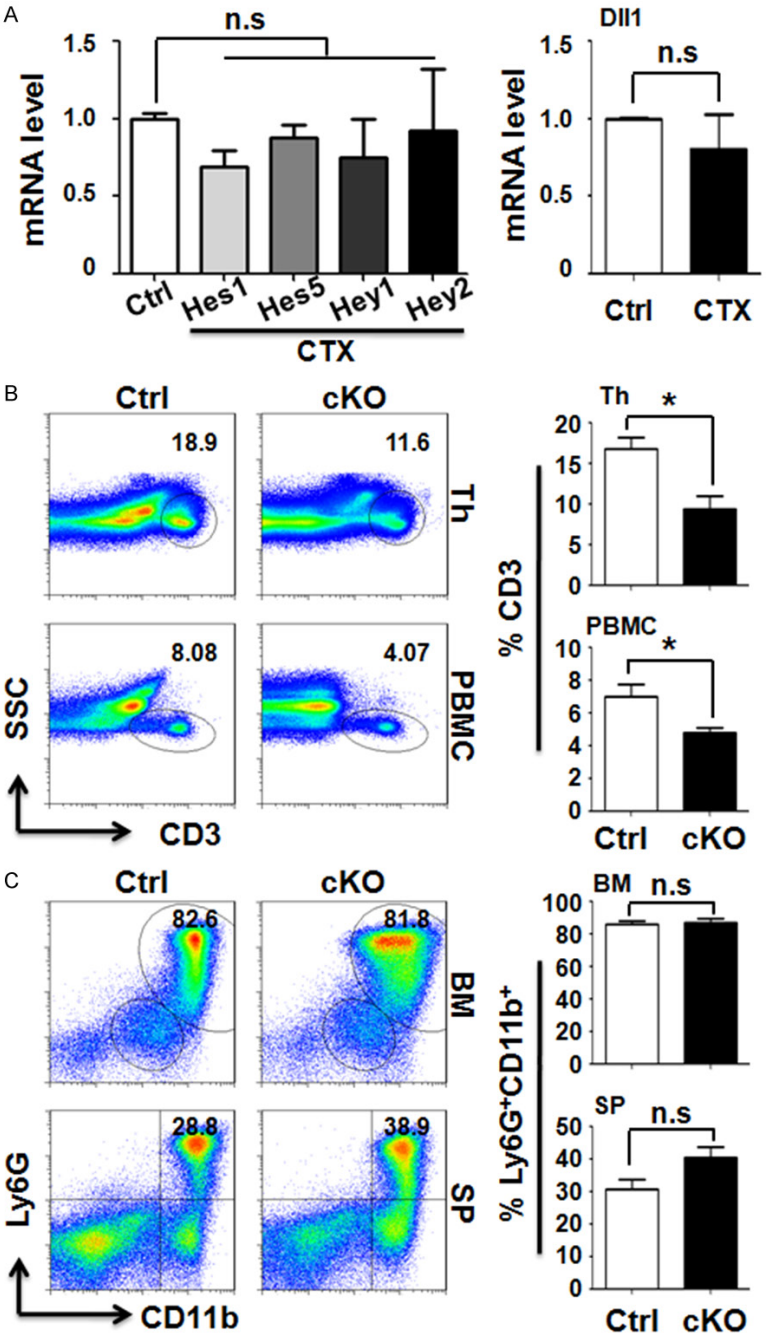

Figure S1. Notch blockade resulted in a block of T cell development. A. 8-week-old C57BL/6 mice were injected with or without CTX intraperitoneally. Three days later, BM Lin^- cells were collected to perform Hes1, Hes5, Hey1, Hey2 (left) and Delta like 1 (right) mRNA expression by qRT-PCR. B. Representative FACS profiles (left) and percentages (right) of thymus (Th) and PB T cells ($CD3^+$) in Mx1-Cre-RBP-$J^{f/f}$ (cKO) and Mx1-Cre-RBP-$J^{f/+}$ (Ctrl) mice 7 days after 150 mg/kg CTX treatment. C. Representative FACS plots (left) and percentages (right) of BM and spleen myeloid cells ($Ly6G^+CD11b^+$) in cKO and Ctrl mice 7 days after CTX. Data are presented as the means ± SEM (n=6). *P < 0.05, n.s P > 0.05 vs Ctrl.

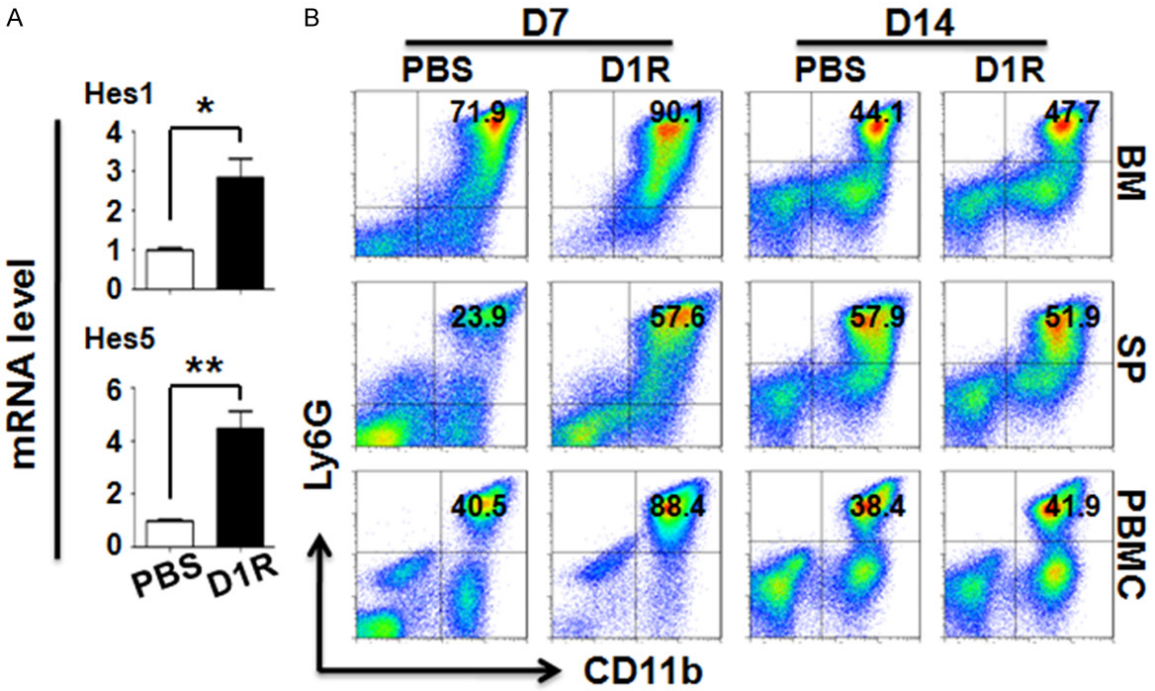

Figure S2. Notch promotes BM reconstitution following CTX. 8-week-old C57BL/6 mice were daily injected with D1R (4 mg/kg) or equivalent PBS for 14 days following CTX treatment. A. Hes1 and Hes5 mRNA expression in sorted BM LSK cells at 3 days after CTX. B. Representative FACS profiles of BM, spleen and PB myeloid cells ($Ly6G^+CD11b^+$) on days 7 (D7) and 14 (D14) post CTX exposure. Data are presented as the means ± SEM (n=6). *P < 0.05, **P < 0.01 vs PBS.

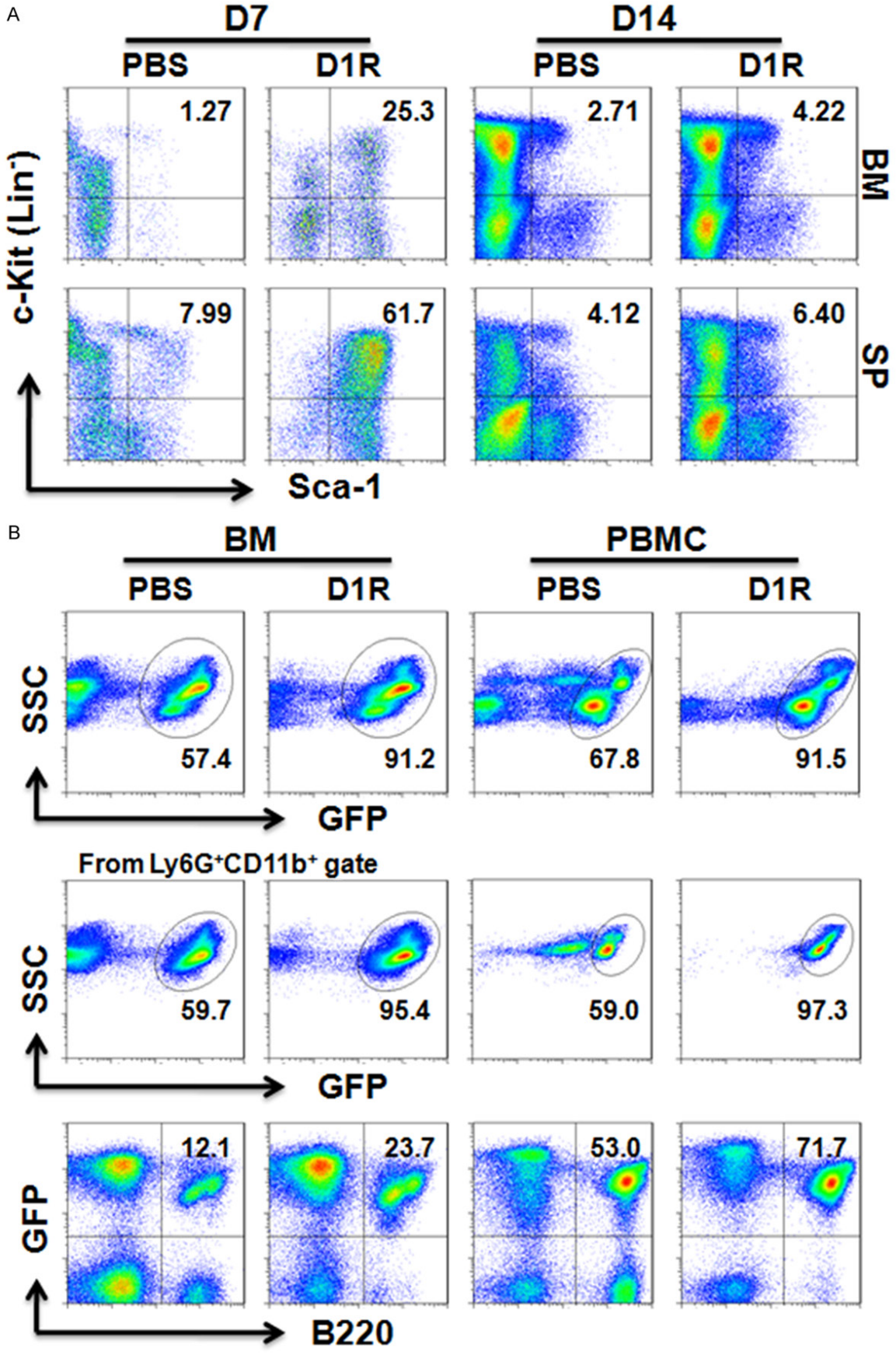
A
D7
D14
PBS
D1R
PBS
D1R
1.27
25.3
2.71
4.22
BM
7.99
61.7
4.12
6.40
SP
c-Kit (Lin-)
Sca-1
B
BM
PBMC
PBS
D1R
PBS
D1R
SSC
57.4
91.2
67.8
91.5
GFP
From Ly6G+CD11b+ gate
SSC
59.7
95.4
59.0
97.3
GFP
GFP
12.1
23.7
53.0
71.7
B220

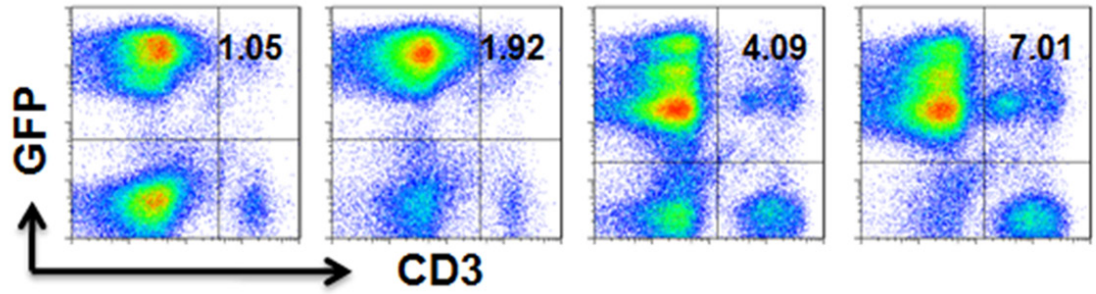

Figure S3. Notch improves HSC regeneration following CTX. A. Representative FACS plots of LSK cells in marrow and spleen 7 (D7) and 14 days (D14) after CTX chemotherapy (n=6). B. Representative flow cytometric analysis of donor GFP$^+$ nucleated cells, myeloid (Ly6G$^+$CD11b$^+$), B-cell (B220$^+$) and T-cell (CD3$^+$) in the BM and PB of recipient mice at 8 weeks following competitive bone marrow transplantation (n=8).

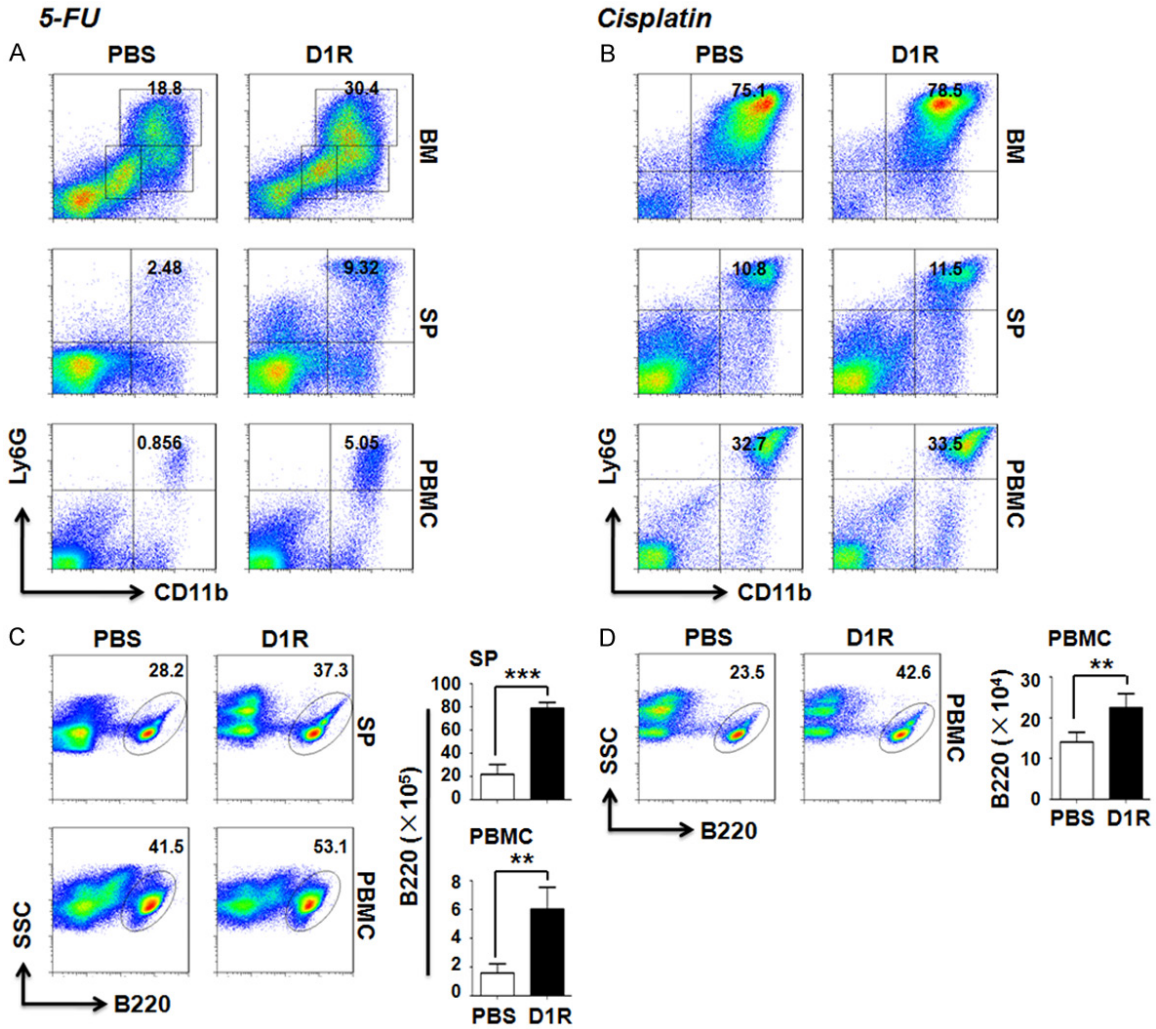

Figure S4. Notch signaling restores hematopoiesis after 5-FU and cisplatin injury. 8-week-old C57BL/6 mice were intraperitoneally injected with PBS or D1R daily for 7 days post 5-FU (150 mg/kg) or cisplatin (5 mg/kg) chemotherapy. (A, B) Representative FACS profiles of marrow, spleen and blood myeloid cells (Ly6G$^+$CD11b$^+$) from PBS- or D1R-treated mice following 5-FU (A) or cisplatin (B). (C) Representative plots (left) and numbers (right) of spleen and PB B cells (B220$^+$) after 5-FU treatment. (D) Representative FACS plots (left) and numbers (right) of B cells (B220$^+$) in PB following cisplatin. Data are presented as the means ± SEM (n=6). $^{**}P < 0.01$, $^{***}P < 0.001$ vs PBS.

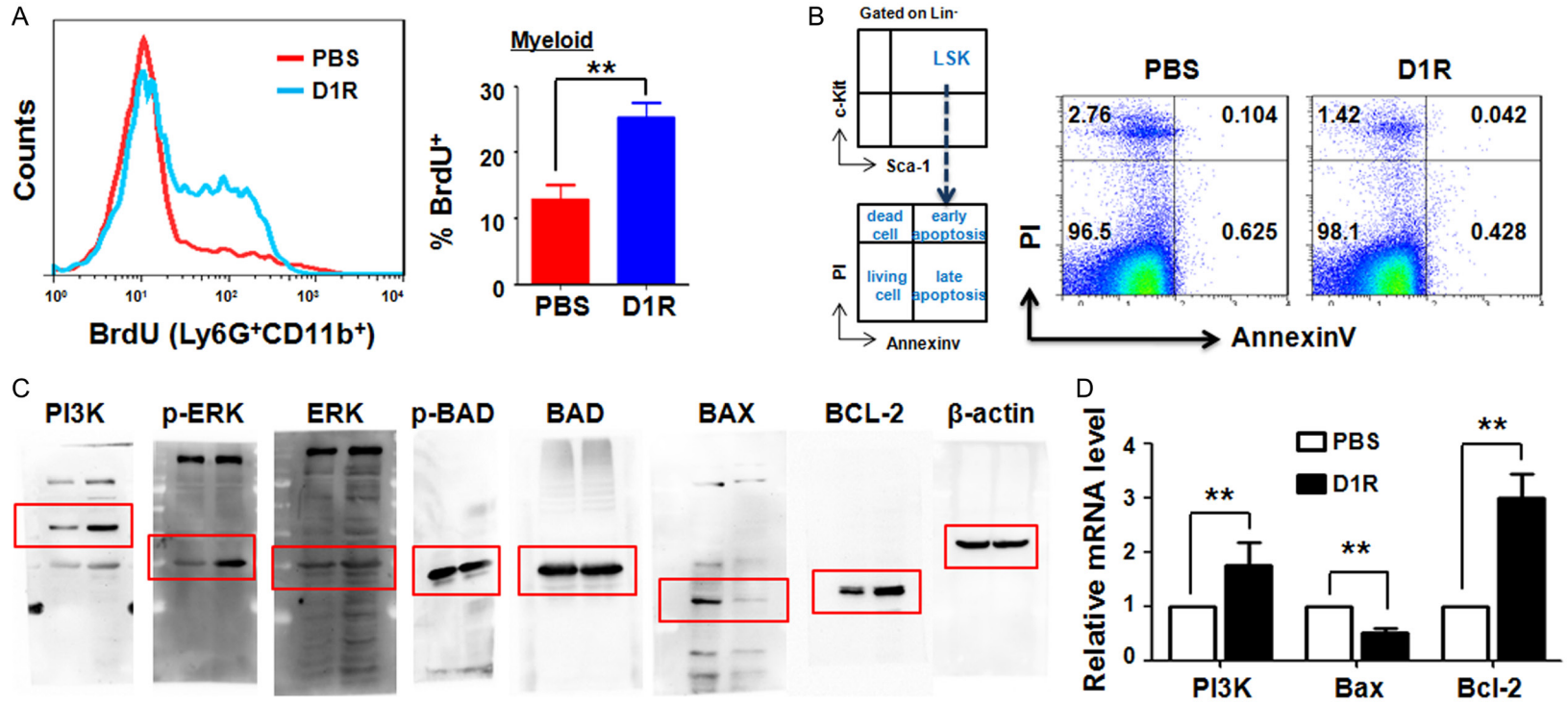

Figure S5. Notch mediates HSCs proliferation. 8-week-old C57BL/6 mice were daily injected with PBS or D1R for 7 days after CTX exposure. A. Representative plots (left) and percentages (right) of BrdU-retaining myeloid precursor cells ($Ly6G^+CD11b^+$) in marrow. B. Representative FACS profiles of BM apoptotic LSK cells. C. Western blot original whole membranes of PI3K, Erk1/2, pErk1/2, Bad, pBad, Bax, Bcl-2 and β-actin in sorted BM LSK cells. D. PI3K, Bax and Bcl-2 mRNA expression in LSK fractions by qRT-PCR. Data are presented as the means ± SEM (n=4). $^{**}P < 0.01$ vs PBS.

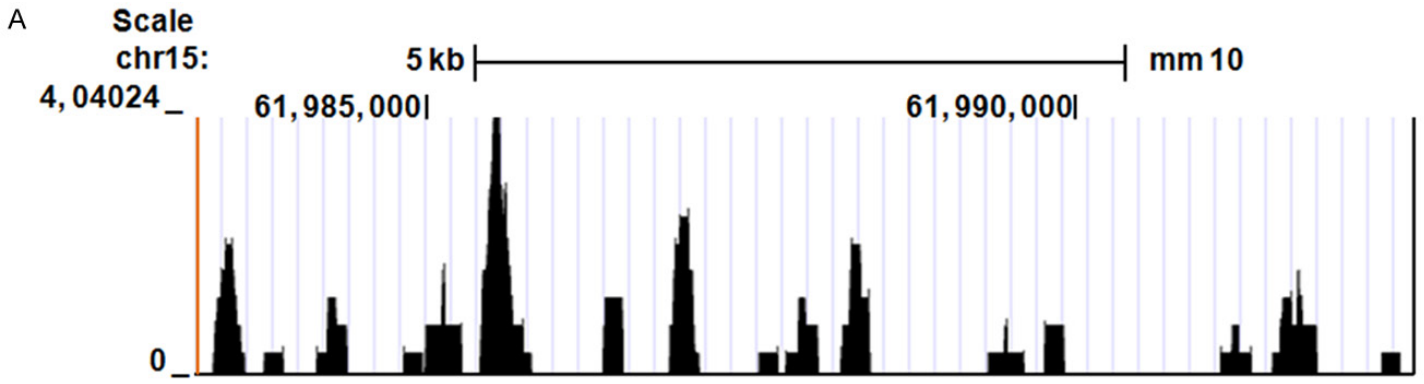

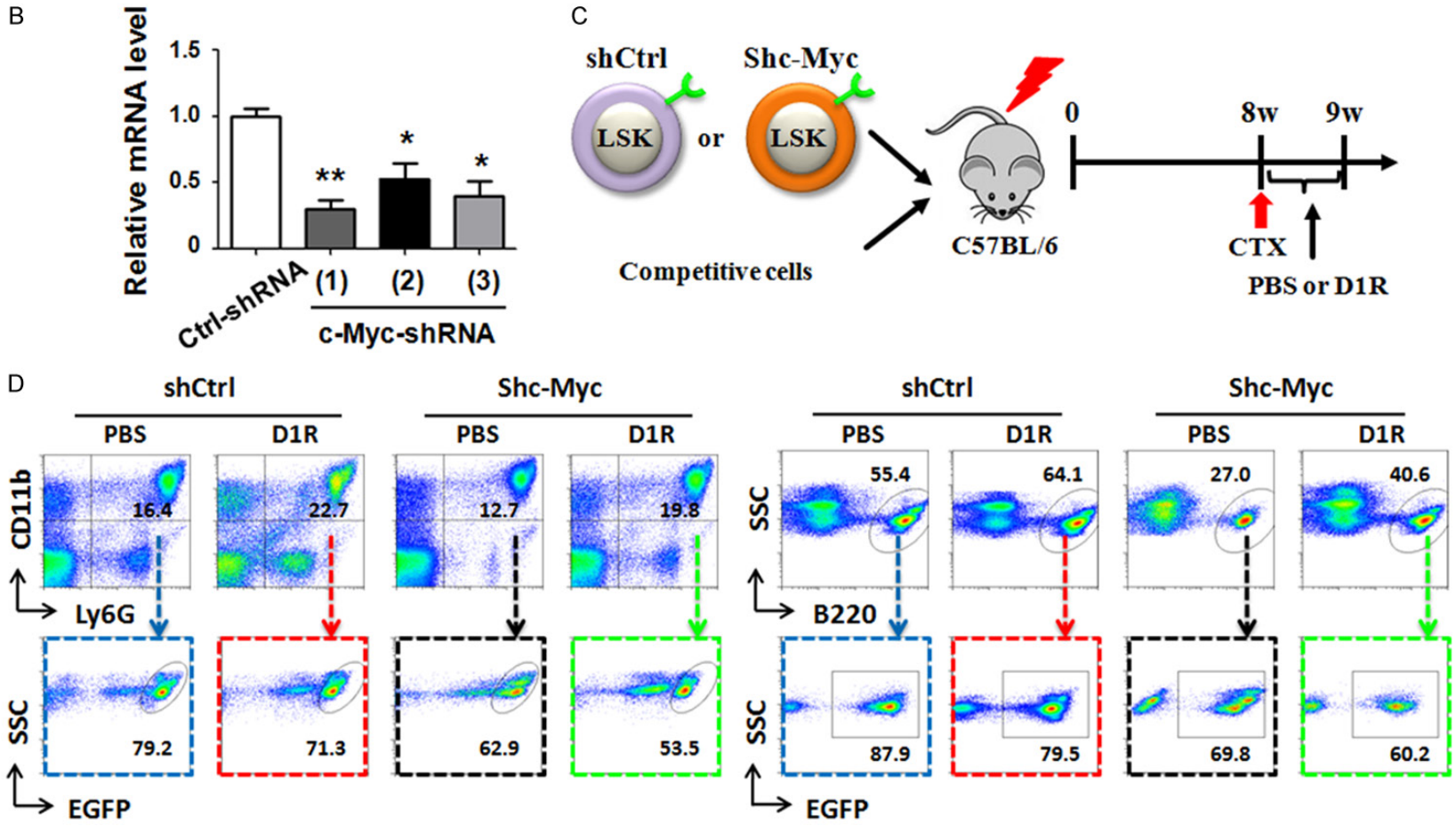

Figure S6. Notch facilitates hematopoietic reconstitution in response to c-Myc. A. Chromatin localization peaks of RBP-J-binding sites (TGGGAA) on c-Myc gene promoter in mouse, using an existing in silico analysis of chromatin immunoprecipitation followed by sequencing dataset. B. Knock down of c-Myc expression using lentivirus-mediated shRNA transfection. C57BL/6 mice BM LSK cells were transfected and cultured with three different shRNAs targeted c-Myc, followed qRT-PCR 7 days later. C. Schematic representation of lentivirus transfection Ctrl-shRNA-EGFP (shCtrl) or c-Myc-shRNA-EGFP (shc-Myc) and hematopoietic stem cell transplantation. D. Representative flow cytometric analysis of PB myeloid- and B-cell engraftment on weeks 9 post-transplantation. Data are presented as the means ± SEM (n=6). $*P < 0.05$, $**P < 0.01$ vs Ctrl-shRNA.